ADVANCED NANOIMPRINT TECHNIQUE FOR MULTILAYER STRUCTURES AND FUNCTIONAL POLYMER APPLICATIONS

A Dissertation

by

HYUNSOO PARK

Submitted to the Office of Graduate Studies of
Texas A&M University
in partial fulfillment of the requirements for the degree of

DOCTOR OF PHILOSOPHY

May 2009

Major Subject: Electrical Engineering

ADVANCED NANOIMPRINT TECHNIQUE FOR MULTILAYER STRUCTURES AND FUNCTIONAL POLYMER APPLICATIONS

A Dissertation

by

HYUNSOO PARK

Submitted to the Office of Graduate Studies of
Texas A&M University
in partial fulfillment of the requirements for the degree of

DOCTOR OF PHILOSOPHY

Approved by:

Chair of Committee,	Xing Cheng
Committee Members,	Mosong Cheng
	Arum Han
	Kenith Meissner
Head of Department,	Costas N. Georghiades

May 2009

Major Subject: Electrical Engineering

ABSTRACT

Advanced Nanoimprint Technique for Multilayer Structures and Functional Polymer Applications.

(May 2009)

Hyunsoo Park, B.S., Kyungpook National University;

M.S., University of Florida

Chair of Advisory Committee: Dr. Xing Cheng

Three-dimensional (3D) polymer structures are very attractive because the extra structural dimension can provide denser integration and superior performance to accomplish complex tasks. Successful fabrication of 3D multilayer microstructures in thermoplastic polymers using optimized nanoimprint lithography techniques such as layer-transfer and transfer-bonding methods are developed in this dissertation work. The capability and flexibility of the techniques developed here are expected to have deep impact on the applications of soft materials such as polymers including functional polymers in micro- and nanofabricated devices and systems. Although NIL technique is developing rapidly in recent years, there are still issues that need to be addressed for broader adoption of the nanoimprint technique. One of the problems is the residual layer that remains in the polymer pattern after nanoimprint. The conventional approach, oxygen reactive-ion-etching (RIE) process, to remove the residual layers, increases the cost and lowers the overall throughput of the nanoimprint

process. More severely, it can degrade or even damage the functional polymers. In order to overcome these problems, new residual layer removal techniques need to be developed. In this dissertation, two methods are newly developed, which do not negatively affect the chemistry of the polymer materials. The techniques are suitable for all thermoplastic polymers, particularly functional polymers.

Another advantage of nanoimprint is its ability to directly create functional polymers structures. This is because thermal nanoimprint only needs temperature and pressure for pattern replication, which both are benign to functional polymers. This feature combined with newly developed techniques such as transfer-bonding and residue removal techniques opens up the possibilities in nondestructive functional polymers patterning at the micro- and nanoscale for novel applications in electronics, optoelectronics, photonics and bioengineering.

Finally, several applications of 3D multilayer structures fabricated by the techniques developed in this dissertation are demonstrated. The first application is a multilayer metal-dielectric-metal structure with embedded microfluidic channels. This structure can be used as an on-chip tunable filter for integrated microfluidic applications. The second application is a multilayer microfluidic channels in which each layer has a different channel size. This device can be used for particle separation and filtration based on lateral fluid flow.

To My Parents

ACKNOWLEDGEMENTS

Foremost, I want to express my deep respect and gratefulness to my advisor, Dr. Xing Cheng, who led me to the way of learning and took care of me with love. Dr. Cheng's enthusiastic support and invaluable advice kept me on track toward developing this research. Appreciation is also given to the committee members, Dr. Mosong Cheng, Dr. Arum Han and Dr. Kenith Meissner, for their critical comments and valuable suggestions. Without my committee members' constant guidance, the dissertation would not have been possible.

I have been blessed to know so many people in the Department of Electrical Engineering who have been helpful and supportive during my time at Texas A&M. My special thanks go to my colleagues who have helped me with discussions and friendship, Huifeng, Dehu and Patrick. I am also very thankful to my extended family of alumni of Kyungpook National University and the Vision Mission Church for their friendship and support.

From deep in my heart, I would like to give my special thanks to my parents, my wife and son, Hyejin and Nicholas, for their sacrifice, devotion, support, encouragement and endless love throughout this research.

TABLE OF CONTENTS

CHAPTER Page

CHAPTER Page

LIST OF FIGURES

FIGURE Page

FIGURE Page

FIGURE Page

FIGURE Page

LIST OF TABLES

CHAPTER I

INTRODUCTION AND PRINCIPLES OF NANOIMPRINT LITHOGRAPHY

Nanotechnology has made significant progress since Richard Feynman introduced the idea in a 1959 with a lecture entitled "There's Plenty of Room at the Bottom" although he did not use the word "nano". Nanotechnology refers to a field whose theme is the control of matter on an atomic and molecular scale. Generally, nanotechnology deals with structures of one dimension less than 100 nanometers. A nanometer is a unit of spatial measurement, one billionth of a meter (10^{-9} meter) in diameter. In this range, materials and devices can be created with valuable properties, which enable us to use it for better life. Figure 1 shows the different sizes of some materials [1]. For example, the human hair is 10,000 to 50,000 nm and DNA is typically 2 nm.

According to Moore's law, the number of transistors on chips doubles every 18 months as manufacturing abilities for nanotechnology have been rapidly developed during last two decades [2]. Today, it is possible to integrate one billion transistors in one square inch of silicon wafer with current technology. The 45 nm technology is currently the most advanced technology, which enables us to fabricate the 32 nm DRAM half pitch pattering. Not only varieties of techniques are developed to improve

---

This dissertation follows the style of *Advanced Materials*.

photolithography resolution, tremendous efforts are also contributed to new concept of lithography systems for 32 nm node and beyond. Current lithography techniques considered by microelectronic fabrication include immersion photolithography, extreme ultraviolet lithography (EUV), electron-beam lithography (EBL) and ion-beam lithography (IBL), various maskless lithography techniques, and nanoimprint lithography (NIL).

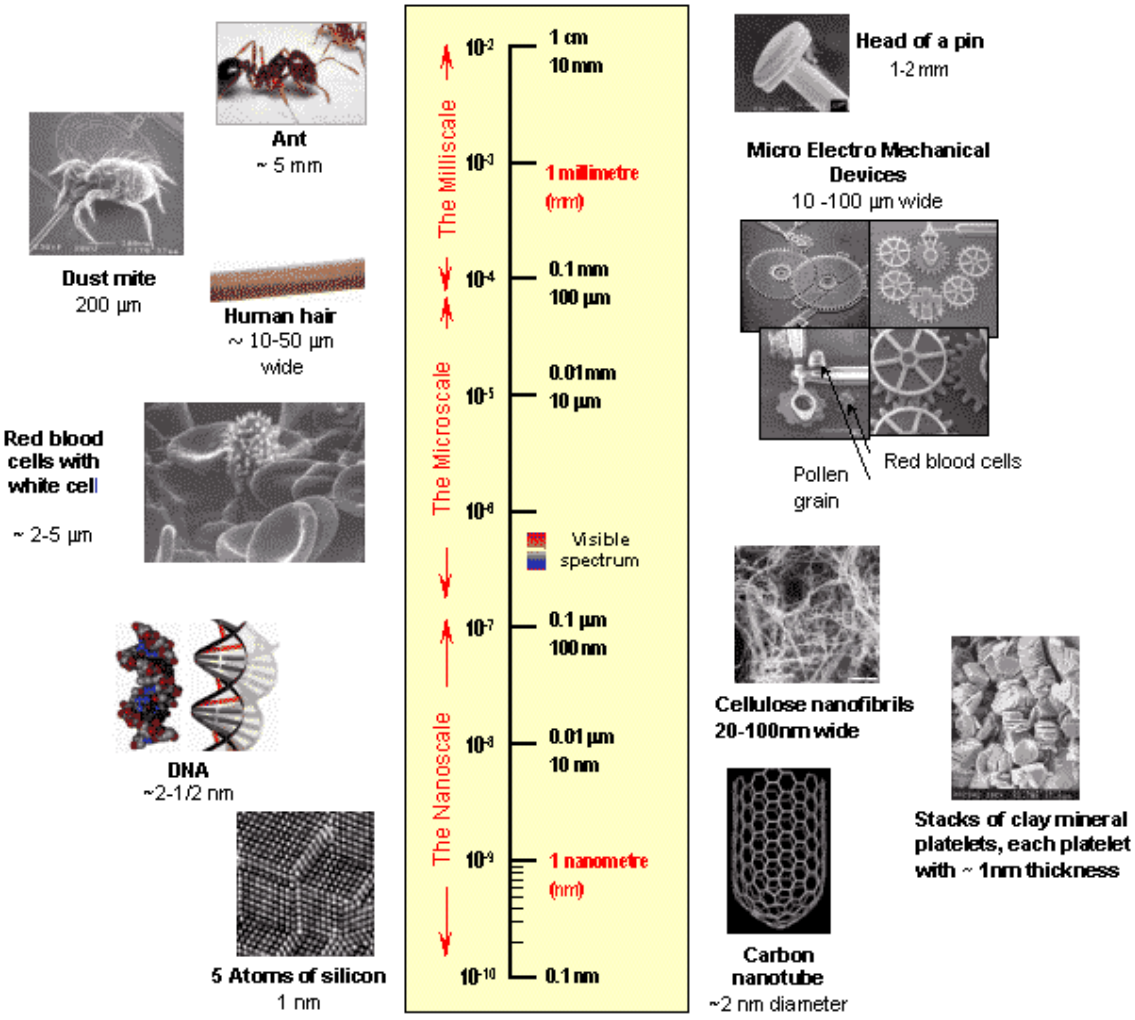

Figure 1. Comparison of the different sizes of materials [1].

1.1 Conventional lithography

Lithography is a compound word of Latin's lithos (stone) and graphos (drawing). This has been used for art and printing areas and currently become essential technique for semiconductor industry as "photolithography", which enable us to integrate huge number of circuits on small chip. Photolithography can be defined the process of transferring geometric shapes on a mask to the surface of a silicon wafer. Figure 2 shows general process of photolithography fabrication process [3]. The processes involved in photolithography are wafer cleaning, photoresist application, soft baking, mask alignment, exposure, development and hard-baking. Currently, the resolution with this technique reaches down to 32 nm.

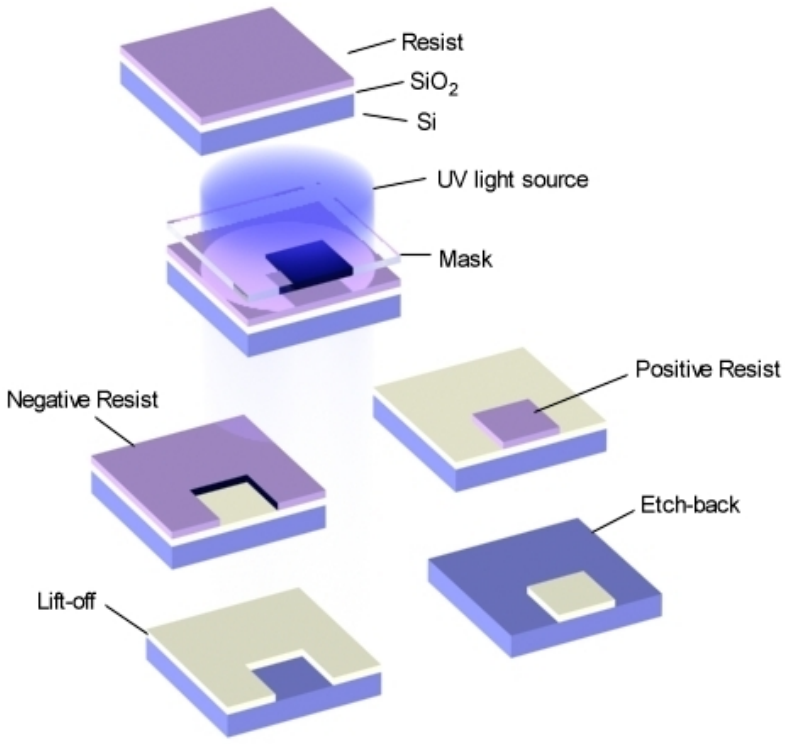

Figure 2. The main processes in photolithography [3].

Despite rigorous development in conventional photolithography such as phase-shift masks, immersion techniques and double patterning, conventional photolithography is almost reaching its limitation. The main limitation is that the wavelength of light used for lithography (currently ArF, 193 nm). Eventually, reduction of the wavelength of the light source is required to achieve a higher resolution. EUV chooses 13.5 nm radiation for lithography. EUV has attracted huge attention as a candidate for next generation lithography. But, there are critical technical issues remain to be solved. First of all, defect-free, smooth, reflective mirrors and masks are needed, which are very difficult to achieve. The second one is the lack of a EUV light source with enough power for high-throughput production. EUV system needs 100W power to have a 100 wafer per hour (WPH) throughput, but current EUV tools can generate only a quarter of it. The third limitation is the photoresist for EUV. EUV photoresists need to have both properties of optical and electron beam resists because EUV photons generate secondary electrons. The resolution can be limited by backscattering of secondary electrons rather than the diffraction limit imposed by the wavelength of the light source.

Alternatively, there are couples of other lithography techniques such as EBL, X-ray lithography (XRL), IBL and focused ion beam lithography (FIB). Each technique has its own unique advantages and disadvantages. For example, the EBL has very high resolution but very poor throughput X-ray lithography is facing even bigger challenge than EUV due to shorter wavelengths. It remains unclear whether

those lithography techniques can overcome their problems to become a mainstream technology used in microelectronic industry.

1.2 Soft lithography

Since Prof. Whitesides group at Harvard University introduced soft lithography at early 1990's, enormous researches have been done in this area [4, 5]. Soft lithography can be defined as fabrication of micro- and nanostructure based on replicating by soft, elastomeric mold such as most notably poly(dimethylsiloxane) (PDMS). Based on process details, soft lithography can be categorized into microcontact printing (μCP) [6, 7], replica molding (REM) [8], microtransfer molding (μTM) [9], micromolding in capillaries (MIMIC) [10] and solvent-assisted micromolding (SAMIM) [11]. The schematic illustration of each technique is shown in Figure 3 [5].

In soft lithography, the elastomeric mold is the key element which transfers patterns onto the substrate. This elastomeric mold can be prepared by replica molding. A prepolymer of elastomer is poured over a master having a patterned relief structure on its surface, then cured and peeled off. The most commonly used elastomeric material is PDMS. The PDMS has unique properties to become a good template material for soft lithography. It is deformable enough on microscale nonplanar substrate due to its elastic characteristic, so that PDMS can make conformal contact with substrate. PDMS is also chemically stable, optically transparent and hydrophobic, which make it attractive for many applications. However, due to its low Young's

modulus, it is very difficult to replicate structures of sub-100 nm by PDMS templates. Although PDMS microcontact printing can find numerous applications in chemical and biological engineering, it is not very useful for microelectronic fabrication.

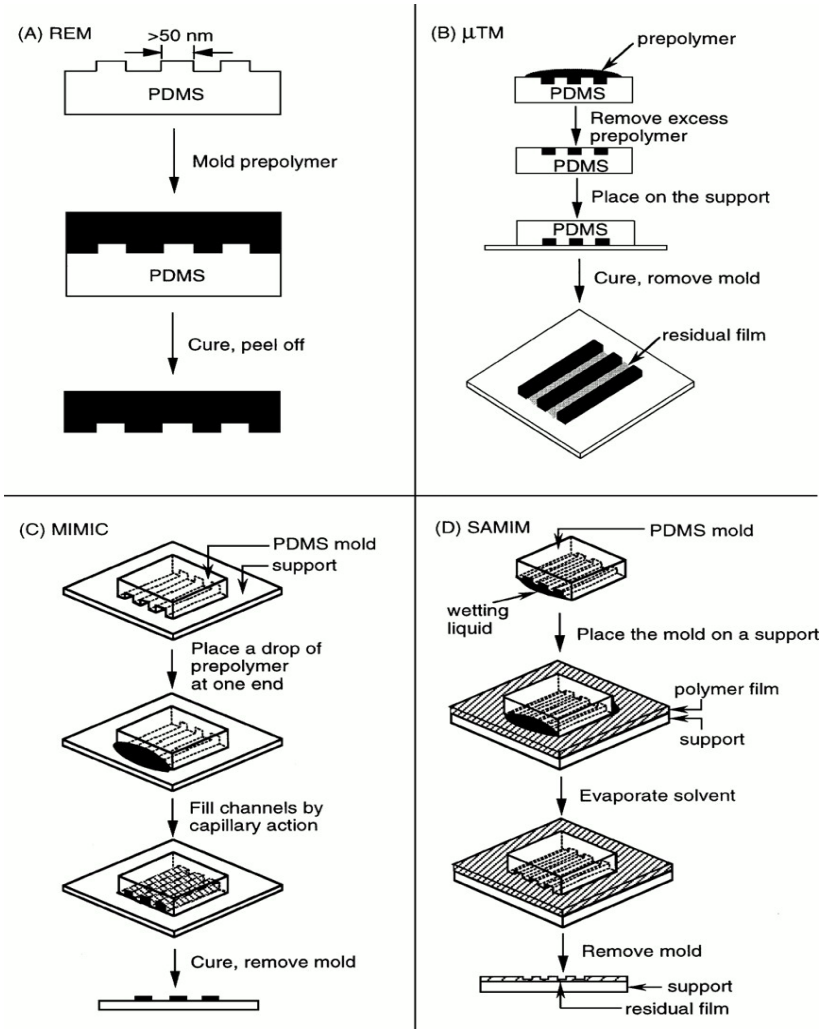

Figure 3. Schematic illustration of procedures for (a) replica molding (REM), (b) microtransfer molding (μTM), (c) micromolding in capillaries (MIMIC), and (d) solvent-assisted micromolding (SAMIM) [5].

1.3 Nanoimprint lithography

Nanoimprint lithography (NIL) has received a huge amount of attention as a strong candidate for next generation lithography system since it has been developed in 1995 by Stephen Y. Chou [12]. Figure 4 shows the schematic of the originally proposed NIL process. It is a very simple process and can be simply defined as a mechanical forming technique that physically molds a deformable material into desired shape. A hard mold that contains nanoscale surface relief features is pressed into a polymer material cast on a substrate at controlled temperature and pressure, which creates thickness contrast in the polymer material. A thin residual layer is left underneath the mold protrusions acting as a soft cushion layer that prevents direct impact of the hard mold onto the substrate, which effectively protects the delicate nanoscale features on the mold surface. In most of the applications this residual layer needs to be removed by an anisotropic oxygen plasma reactive-ion-etching (RIE) process to complete the pattern definition.

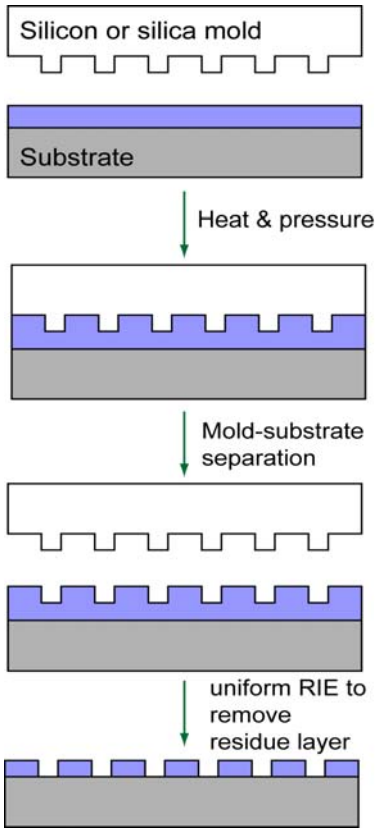

Figure 4. A schematic of nanoimprint lithography.

Not only sub-10 nm resolution [13] but also low cost and high throughput characteristics enable NIL to become a one of the strong candidates for next generation lithography (NGL) method at 32 nm node and beyond as shown in Figure **5**. This figure shows how the lithographic options vary as the critical device dimension decreases, and provides estimates of the timescales on which decisions may need to be made regarding which options to adopt [14].

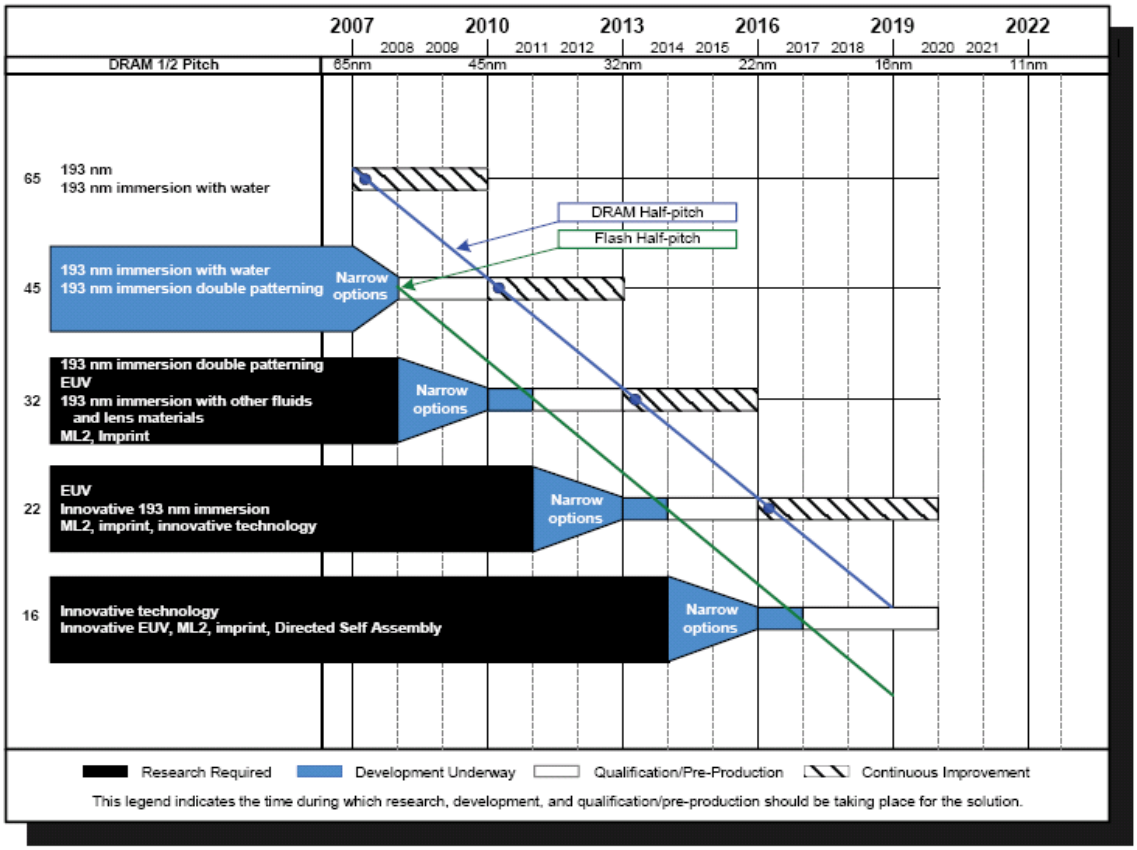

Figure 5. The international technology roadmap for semiconductors (ITRS) in 2008 [14].

Based on materials used in imprint, there are two main streams which are intensively researched. The first one is thermal NIL, which is originally proposed by Stephen Y. Chou. The other method is UV-NIL [15]. Figure 6 shows the comparison of two different methods. The main concept of both methods is same and the only difference is the polymer material. In UV-NIL, a UV curable liquid resist is applied to the substrate and the mold is made of transparent material such as fused silica or

quartz. After the mold and the substrate are pressed together, the resist is cured in UV light and becomes solid.

Both methods have their own advantages and disadvantages. Thermal NIL use high temperature so there is always coefficient of thermal expansion (CTE) mismatch problem and it causes distortion in pattern alignment. UV-NIL uses low temperature which has no CTE mismatch issue without the need for heating and cooling, UV-NIL is a fast process, which is good for mass manufacturing in microelectronics industry. Thermal NIL needs high pressure and consequently it is another source of defect generation due to nonuniformity in pressure. UV-NIL must use a transparent mold, which is an advantage for easy alignment. UV-NIL resists have volume shrinkage problem due to liquid-to-solid phase transition during patterning. One of the biggest advantages of thermal NIL is the availability of resist materials. Many industrial polymers are thermoplastic polymers which mean these materials are only compatible with thermal NIL. Because thermal nanoimprint is capable of pattern any thermoplastic polymers, this provides great freedom in choosing polymers with most appropriate properties for specific applications.

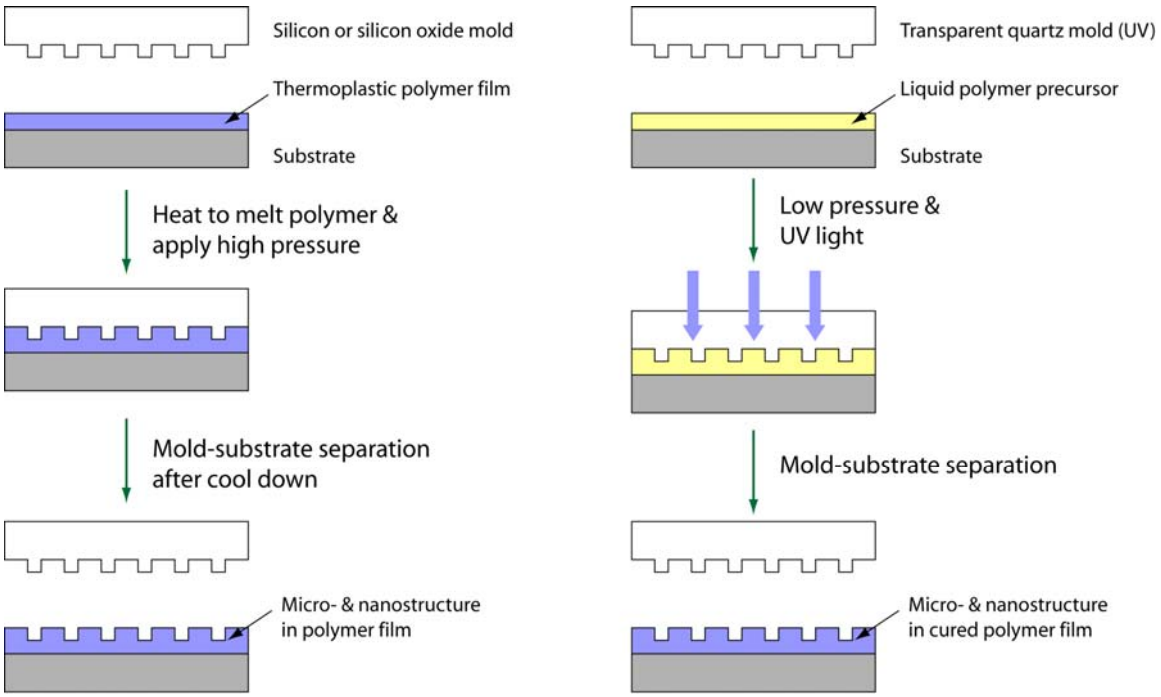

Figure 6. Comparison of thermal NIL (left) and UV-NIL (right).

Since its inception, nanoimprint has received wide-spread attention due to its potential for high-resolution, low-cost and high-throughput nanopatterning. Current nanoimprint development mainly focus on two fronts: 1) developing nanoimprint as a lithography tool for micro- and nanoscale structure and device fabrication; and 2) developing nonconventional nanoimprint schemes and exploring novel applications for nanoimprint techniques.

1.3.1 Nanoimprint mold

Nanoimprint lithography offer the possibility to achieve sub-10 nm features over a large area but it is highly dependent on mold fabrication because NIL is

physical replication of mold pattern. Therefore, the quality of the mold has direct impact on the quality of the imprinted resist. The molds can be fabricated by EBL or FIB for small features, and by conventional optical lithography for relatively large patterns. Figure 7 shows some of the molds fabricated and used for nanoimprint lithography in this dissertation work.

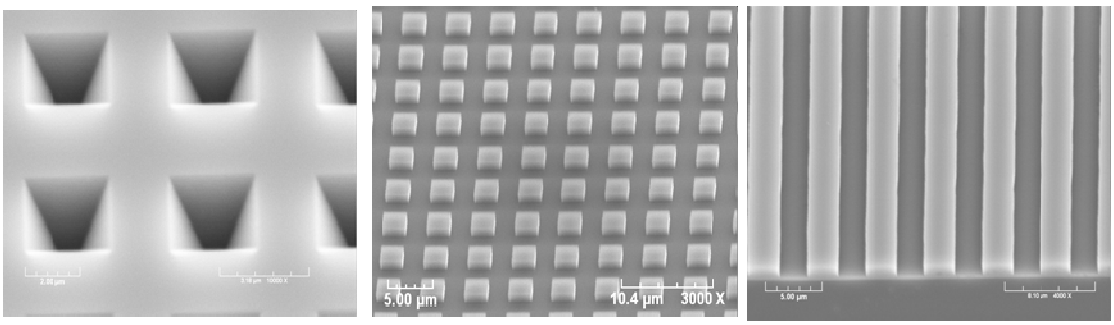

Figure 7. Various type of nanoimprint molds: pyramids (left), dot arrays (middle) and gratings (right).

Hard nanoimprint mold have mostly been made of silicon (Si) or silicon dioxide (SiO_2), while it is also possible to have a variety of choice of material for mold fabrication such as nickel (Ni), diamond [16] and SiC [17]. Silicon is widely available cheap, and a capable of being processed by a variety of etching techniques. The thermal expansion coefficient is also important in thermal NIL, where a temperature cycling over 100^{o}C -200^{o}C is typically required in imprinting step. Thermal mismatch between the mold and the substrate could result in pattern distortions and alignment

errors. In this regard, a Si mold and Si substrate make a very good pair for the NIL process.

Quartz is a common mold or template material for UV-NIL due to its transparency. Nickel is also popular material for NIL due to its popularity in electroplating but nickel mold and silicon substrate have thermal expansion mismatch issue [18]. Diamond thin film prepared by CVD has become an attractive mold material for nanoimprint application that requires very high pressure due to diamond's durability. For low cost and fast prototype applications where pattern resolution is not a stringent requirement, casted thermoset polymers such as cured SU-8, polyurethane and polyimide can also be used [19, 20].

1.3.2 Anti-adhesion coating for nanoimprint molds

Anti-adhesion treatment is widely used in a variety of industry fields. It also becomes an essential process for contact lithography, MEMS, bio-engineering and nano-fabrication. In semiconductor industry, surface treatment of mask for contact or proximity lithography has been used to reduce defects. The mold used for NIL has a high density of protrusion features on its surface, which increase the total surface area that contacts the imprinted polymer and therefore leads to severe sticking problem between the mold and polymer. The solution to this problem is to form the anti-adhesion layer on the mold. Depositing self assembled monolayers (SAMs) on mold surface is the most widely used technique today.

SAMs are formed when one end of the molecules bind to substrate surface while the other end, usually a functional group, exposed to environment as shown in Figure 8 [21]. SAMs can control the chemical functionality and mechanical property of the original surface with variety of functional groups. Once the molecule binds to the surface, it is a chemical bonding (mostly covalent bonding) which makes SAM coating very durable for repetitive nanoimprints [22]. For nanoimprint application, the exposed end of SAM is usually hydrophobic functional groups, such as perfluorinated alkyl chains. Hydrophobic SAM renders mold surface nonsticking, hence polymer adhesion during nanoimprint can be greatly reduced to eliminate pattern defects.

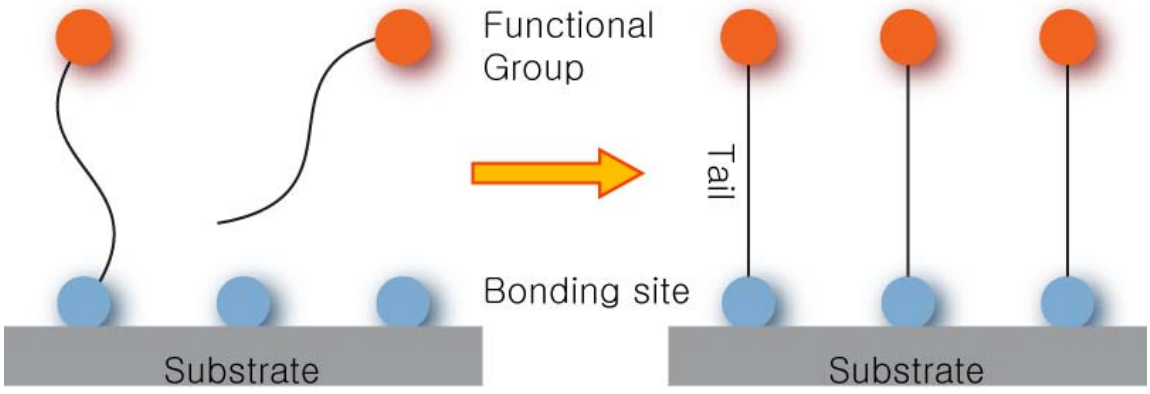

Figure 8. Formation of SAMs from a disordered mass of molecules to a highly ordered monolayer.

Table 1 in below shows relatively popular chemicals for anti-adhesion layer [23].

Table 1. List of typically used surfactants for anti-adhesion SAM coating in nanoimprinting.

Name	Chemical composition	Boiling point	Contact angle
Dichlorodimethylsilane (DDMS)	$C_2H_6Cl_2Si$	70°C	103°
Octadecylmercaptan (ODT)	$C_{18}H_{38}S$	210°C	110°
Undecyltrichlorosilane (DTS)	$C_{11}H_{23}Cl_3Si$	155°C	110°
Octadodecyltrichlorosilane (OTS)	$C_{18}H_{37}Cl_3Si$	220°C	110°
1H,1H,2H,2H-perfluorodecyltrichlorosilane (FDTS)	$C_{10}H_4C_{l3}F_{17}Si$	216°C	120°
Perfluoroctyltrichlorosilane (FOTS)	$C_8H_4C_3F_{13}Si$	192°C	110°
10-Undecenyltrichlorosilane (UTCS)	$C_{11}H_{21}Cl_3Si$	100°C	100°
Perfluorodecanoic Acid (PFDA)	$CF_3(CF_2)_8COOH$	218°C	110°

Among these surfactants, 1H,1H,2H,2H-perfluorodecyltrichlorosilane (FDTS) is the most widely used for anti-adhesion coating [15]. Methods to assemble monolayer on top of the mold are spin coating, solvent coating, vapor coating and plasma polymerization. The most widely used methods for NIL are solvent coating and vapor coating. Each method has its own advantages and disadvantages. Figure 9 shows the how to form a self assembly monolayer of FDTS on substrate using solvent coating method. First of all, the mold is immersed into acid bath mixture of sulfuric acid and hydrogen peroxide in a ratio of 7:3, which is called piranha cleaning process to remove any organic contaminants on mold. Then the mold is heated above 150°C to remove any moisture. After these cleaning process, the real self assembly monolayers coating is started. The surfactant, FDTS, is first mixed with solvent such as heptane. Then, the mold is immersed into the solution for about 10 minutes to form the SAMs. The reaction sequence in the mixed solution starts at the hydroxylation of Si-Cl bonds in FDTS chains. The hydroxyl group (-OH) in surfactant molecules reacts with the –OH group on mold surface and from the -OH group on neighboring surfactant molecules. This is followed by the dehydrolyzation process to form Si-O-Si bonding. Finally, the mold is placed on hot plate to facilitate dehydrolyzation process and remove loosely bonded surfactant molecules. After these processes, a SAM of FDTS are formed on top of the mold surface, which bond to mold surface through strong Si-O-Si bonds.

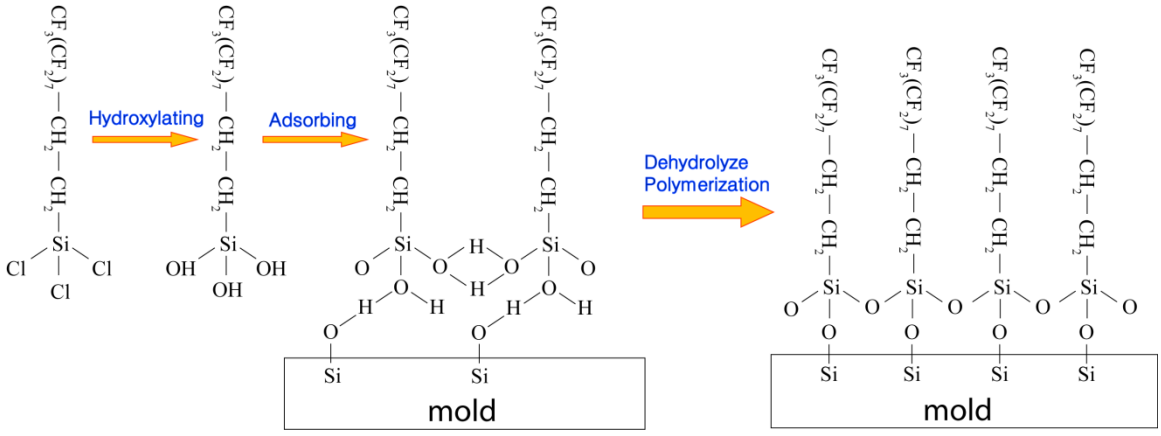

Figure 9. The formation of FDTS SAM on substrate using solvent coating method.

Vapor coating is a much simpler process. After piranha cleaning and baking process, the mold is placed in a vacuum chamber. Surfactant molecules (silanes) are injected into the chamber. The rest of the process is almost same as solvent coating. There are advantages and disadvantages for both methods. Solvent coating method is a low cost process, but coating defects are common, particularly for high-aspect-ratio nanostructures. Figure 10 shows an example about how it happens. For nanostructures, surface tension and air pockets prevent solution from reaching the trench areas, which leaves the trench areas uncoated with surfactant. Another issue is that the mold can become very dirty after solvent coating. As shown in Figure 11, the left picture shows the mold just after solvent coating with FDTS. A lot of residues on top of the mold are clearly seen but after 3 times imprinting process the mold surface becomes clean. This residue is mainly from solution during solvent coating because silane surfactants polymerize in solvent and form particles that eventually precipitate on mold surface. Those particles, or residues, can be removed by nanoimprint because they will be

embedded in polymer resist layer and removed from mold surface after nanoimprint. Such self-cleaning property is another advantage of nanoimprint lithography. On the other hand, vapor coating method is easier to form surfactant SAM regardless of the structure. Some researchers have claimed that vapor phase coating can provide better imprint results for nanoscale features [24]. The disadvantage of vapor coating is that this method requires vacuum system, which incurs higher cost compared to solvent coating method.

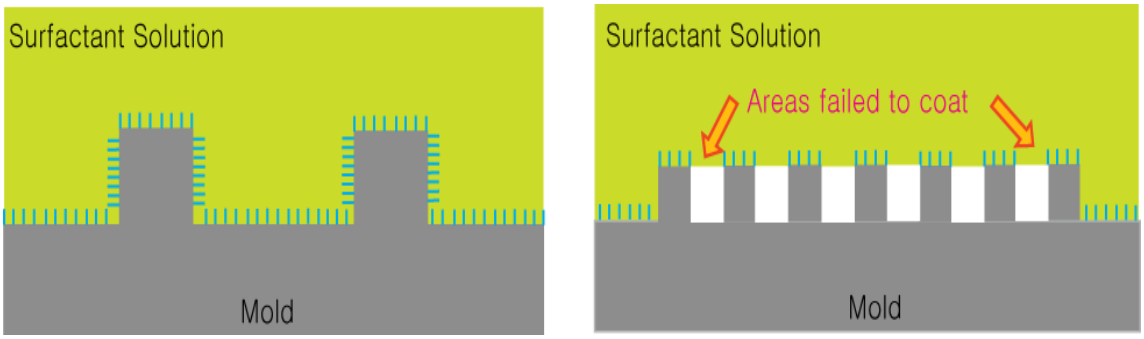

Figure 10. Failure of surfactant coating with solvent coating method.

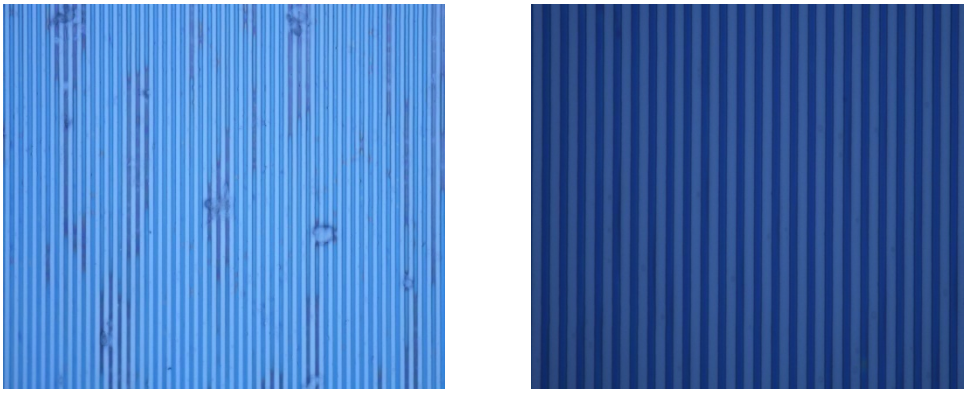

Figure 11. The molds after solvent coating (left) and after 3 times imprinting process (right).

In special situations where mold material itself is a nonsticking material, there will be no need for mold surfactant coating. Recently, amorphous fluoropolymer has been proposed, such as Teflon AF (T_g= 240^{o}C), to be used as an imprinting mold without any surface treatment. Teflon AF mold is prepared by casting the fluoropolymer solutions over a prefabricated template and drying off the solvent [25] or by direct imprinting of this fluoropolymer at 350^{o}C at a high pressure [26].

1.3.3 Resist materials for nanoimprint lithography

Polymer material is a very good choice for many applications particularly in the bio-engineering field because of their lower cost and biocompatibility. Understanding the mechanical properties of polymer is important to control the NIL process. Polymer is between ideal metal (elastic material) and ideal liquid (viscous material) which means polymer is viscoelastic material. Upon heating, polymers exhibit distinct regions of viscoelasticity. Figure 12 shows the five different regions of viscoelasticity in a polymer. The polymer exists in glassy region at low temperature. In this region, the modulus of elasticity is high (10^9 Pa) so that polymer is stiff. The thermal energy in this region is not enough for polymer molecules to overcome energy barrier, so called frozen state, and only small oscillation of polymer segment is possible around original position. As temperature increases, this oscillation is getting bigger and thermal energy reaches to the energy barrier for enough parallel or circular movement, which is called the glass transition region. In this region, the modulus of elasticity is decreasing rapidly by more than 1000 times so that the polymer becomes

soft and moldable. Usually this region spans over 10-20°C. The polymer exhibits both rubbery and flow characteristics in the rubbery flow region at a temperature above the glass transition region. Finally, in the liquid flow region at even higher temperature, the polymer can flow like a liquid. If the polymer is crosslinked sufficiently, it doesn't soften, but follows the dotted line. If the polymer is semi-crystalline, it usually has a melting point at much higher temperature.

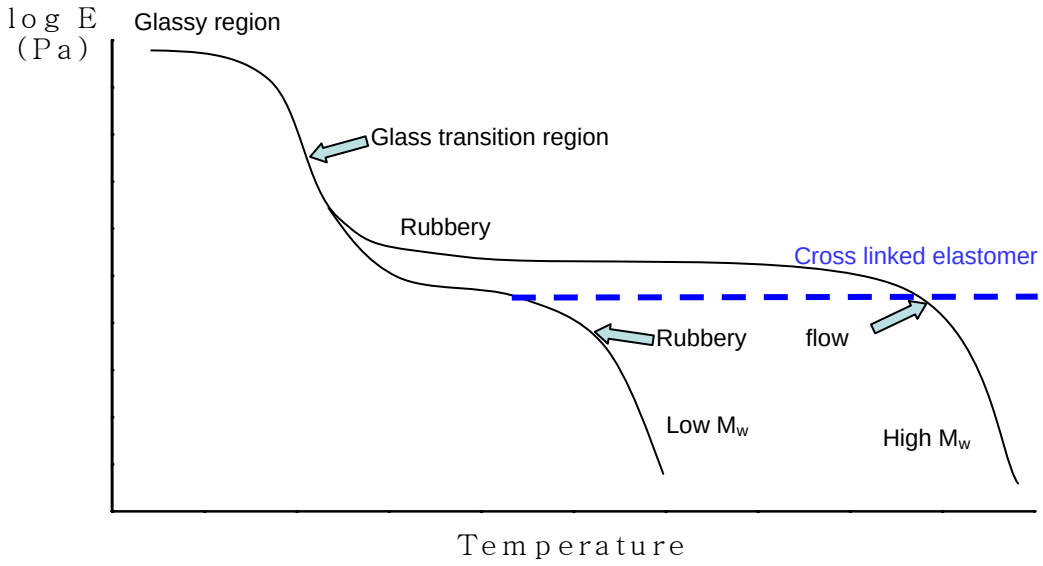

Figure 12. The five regions of polymer viscoelasticity.

Nanoimprint is a mechanical deformation technique to replicate the mold structure onto deformable structure. For high quality pattern replication, the polymer resist should be well deformable under applied pressure to make a desired structure. To reduce imprint time for higher throughput, it would be desirable to have an amorphous thermoplastic with a lower glass transition temperature to reduce waiting

time for heating and cooling. Additionally, the polymer should be stable up to the imprint temperature. The hydrophobic property is also desirable for better demolding process. Good mechanical strength is also needed to maintain its structural integrity during demolding process.

Depending on their physical properties, polymers for NIL can be used for different purposes. For example, polymers used as sacrificial mask layer need to be durable for dry etching. High M_w. semi-crystalline polymer is desirable for this purpose. Polymers used for pattern lift-off need to be soluble in solvent. Lastly, specialty polymers with unique properties can remain in the final device as active components after imprinting. Those polymers include functional polymers that combine multiple physical properties, such as mechanical, electrical, optical, acoustic, magnetic and chemical properties, in one place. For example, conducting polymers, piezoelectric polymers, bio-functional polymers and nonlinear optical polymers are all functional polymers. Since the functional polymers are thermoplastic polymers, thermal nanoimprint allows them to be patterned for a lot of novel applications.

1.3.4 Nanoimprint applications

As a generic lithography technique, NIL can be used for a lot of areas such as patterned media, bio chips, polymer waveguides, photonic crystals, micro-ring resonators, nanofluidic devices and nanoelectronic devices. NIL is already getting out of laboratory and getting adopted by industry. The earliest mass applications are patterned magnetic media and nanooptical devices. Figure 13 shows how Hitachi

fabricates ultra-dense patterned magnetic media with NIL [27]. Nanoscale optical devices use subwavelength structures to manipulate optical radiation. Wire grid polarizer is increasingly adapted in micro display projection TV as a core optical component. Normal NIL or roll-to-roll (R2R) NIL can be used to fabricate this device with high throughput and low cost [28, 29].

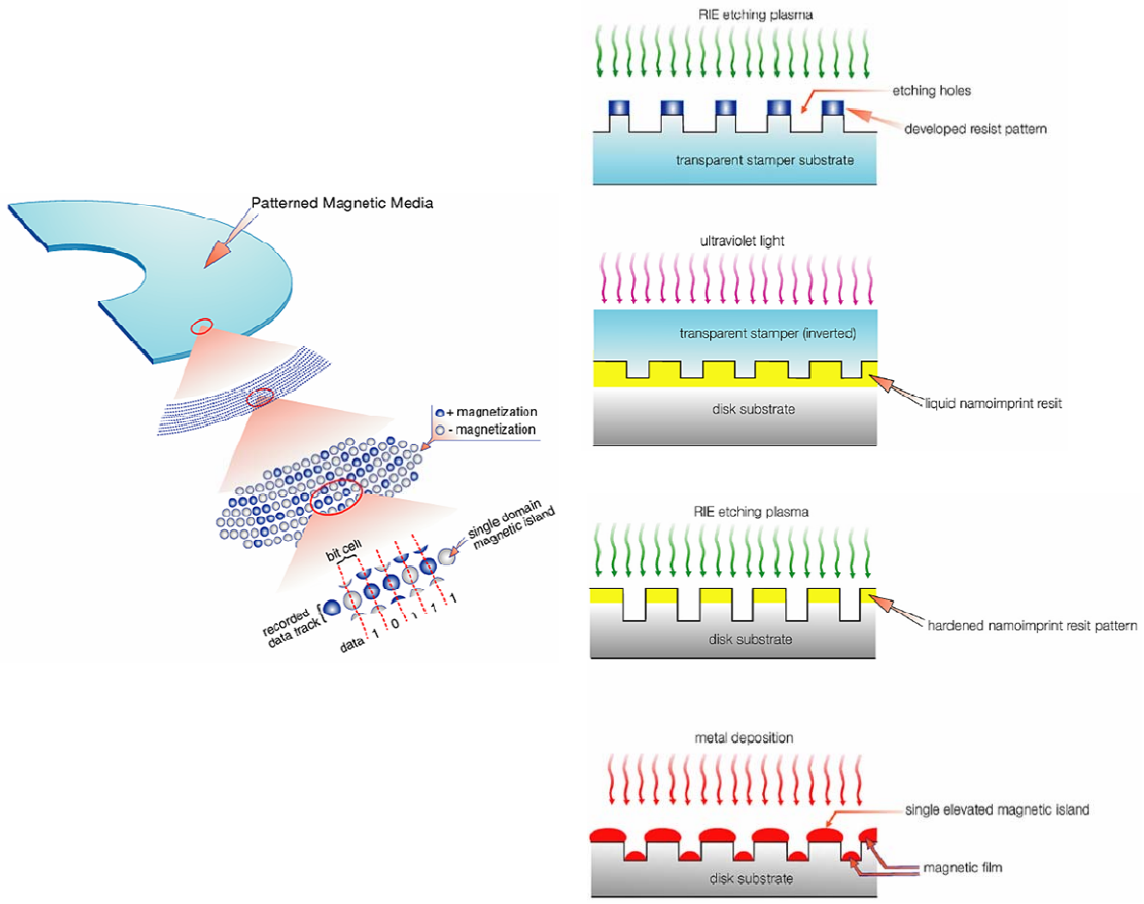

Figure 13. Patterned magnetic media by NIL [27].

1.3.5 Other issues

There are remaining issues for nanoimprint lithography to become a mainstream technique for mass production. The first significant issue is overlay accuracy in pattern registration. The accuracy of the alignment is affected by the mold size, the thermal/mechanical durability of polymer during alignment and the material property of the stamp/substrate. Typical overlay accuracy of optical alignment is around a few hundred nanometers. The Piezo-drive technology could reduce the limit to about 30 nm [30]. Recently, the alignment by matching gratings on mold and substrate has been proposed with alignment accuracy of less than 10 nm. For short-term application, single layer applications such as patterned media and diffractive optical devices will be dominant due to their simplicity.

Another issue in nanoimprint for commercial manufacturing is the defect control since nanoimprint is a physical molding technique that is Prone to defect generation. Particles on wafer before imprinting process should be removed as well as the defect from mold-polymer contact during imprinting should be minimized.

1.4 Dissertation objective

Three dimensional polymer structures are attractive in many micro- and nanofabricated devices and systems for applications in electronics, photonics and bioengineering. The extra structural dimension can provide denser integration and superior performance to accomplish complex tasks. There is an increasing trend of using polymer materials and 3D structures in various MEMS applications due to their

light weight, low cost, easy processing, and multiple functionalities. They can be used to build multilevel microfluidic channels, which can integrate more components into a lab-on-a-chip system to increase its functionality. 3D polymer structures on the order of a few microns to sub-microns can be directly used as diffractive optical components such as 3D photonic crystals. 3D polymer structures can also be used as a sacrificial template to fabricate advanced inorganic 3D microstructures. Polymer 3D scaffolds are also popular in biomedical applications such as tissue engineering.

In this dissertation, one of the main research topics is to achieve successful fabrication of 3D multilayer micron- and submicron-scale structures in both thermoplastic and cross-linked polymers using optimized nanoimprint and transfer-bonding techniques. For successful multilayer fabrication, it is very important to control the adhesion between two polymer layers and between the nanoimprint mold and the polymer. The effects of the surface treatment, the pattern sizes, and the nature of the polymer materials on adhesion force and process yield are explored. For different polymer materials, various approaches are developed to achieve good bonding between two polymer layers. The techniques developed in this disseration are very important due to enormous potential applications. By using different polymers or different pattern size and shape in each layer, the multilayer fabrication methods developed in this work allow various combination scenarios, thus provide great flexibility in designing and fabricating 3D multilayer structures for a broad range of applications. Two exemplar applications of 3D multilayer structures are explored in this dissertation research. The first one is a lateral flow particle separation and

filtration device which can sort particles into various size ranges. The second one is a tunable optofluidic device based on metal-dielectric-metal structure.

Although NIL technique is developing rapidly in recent years, there are still issues that need to be addressed for broader adoption of the nanoimprint technique. One of the most critical problems is the residual layer that remains in the polymer pattern after nanoimprint. Conventional approach to remove the residual layer is to use an oxygen RIE process. This extra step increases the cost and lowers the overall throughput of the nanoimprint process. More severely, oxygen RIE can degrade or even damage the functional polymers by breaking the polymer chains with highly energetic oxygen ions. This eliminates the possibility to create isolated functional polymer structures by nanoimprint for device and system applications, particularly in integrated microsystems where good isolations between devices are needed. In order to further lower the cost and enhance the throughput of nanoimprint, and extend nanoimprint to patterning isolated functional polymer micro- and nanostructures, new residual layer removal techniques need to be developed. In this dissertation work, novel methods are developed to nondestructively remove residual layers in nanoimprint. Patterning functional polymers, particularly conjugated polymers, are demonstrated with those techniques. As a consequence of nondestructive residual layer removal, it presents a novel route to pattern functional polymer nanowires by nanoimprint. The techniques developed in this work open up the possibilities in nondestructive patterning of functional polymers at the micro- and nanoscale for novel applications in electronics, optoelectronics, photonics, sensors and bioengineering.

CHAPTER II

OPTIMIZING NANOIMPRINT AND TRANSFER-BONDING TECHNIQUES FOR THREE-DIMENSIONAL POLYMER MICROSTRUCTURES

2.1 Introduction

Three-dimensional (3D) multilayer polymer microstructures have many applications in electronics, photonics and bioengineering. There is an increasing trend of using polymer materials and 3D structures in various MEMS applications due to their light weight, low cost, easy processing, and multiple functionalities. For example, 3D polymer structures can be used to build multilevel microfluidic channels, which can integrate more components into a lab-on-a-chip system to increase its functionality. 3D polymer structures on the order of a few microns to sub-microns can be directly used as diffractive optical components such as 3D photonic crystals [31]. 3D polymer structures can also be used as a sacrificial template to create advanced inorganic 3D microstructures [32, 33]. For this application, it is very desirable to use thermoplastic polymers in these 3D templates because the polymer scaffold can be easily removed by a solvent, unlike thermoset polymers.

Multilayer polymer microstructures in general can be achieved by layer-by-layer stacking techniques [9]. Recently, layer-by-layer techniques have also been developed based on nanoimprint lithography and polymer bonding [34]. Polymers with progressively lower glass transition temperature (T_g) were used to preserve bottom layer structures while new layers were added on top. Although multilayer

structures can be built, the number of layers that can be achieved and the number of polymer materials that can be used with this method are very limited because the polymers in each layer must have progressively lower T_g. Another method to overcome this issue is to use thermoset polymers such as UV-curable materials [35, 36]. After UV-curing, the thermoset polymer will not deform under pressure, thus allow the bottom layer pattern to be preserved while top layers are added. However, unless the polymer layers are eventually used as a permanent structure in the final device, removing cured polymers will be very difficult. Such difficulty greatly limits the usefulness of the 3D multilayer structures based on thermoset polymers, thus it is very attractive to create 3D multilayer structures in thermoplastic polymers. 3D multilayer polymer structures can also be fabricated by direct bonding with a temperature gradient [37]. Multilayer bonding was accomplished between two platens that were kept at two different temperatures. However, precise control of the temperature gradient to prevent bottom layer deformation is very difficult to achieve.

Although 3D polymer multilayer microstructures have many advantages, there are not many applications of them yet, mainly due to the lack of a reliable technique to create those structures, particularly in thermoplastic polymers. In this work, we optimize the nanoimprint and transfer-bonding processes to develop a generic approach to create 3D polymer microstructures with decent to high yield. It is expected that the methods developed in this paper can potentially lead to wide-spread applications of polymer multilayer structures in micro- and nanoscale devices and systems.

2.2 Transfer-bonding of three-dimensional polymer microstructures

The molds used in nanoimprint and transfer-bonding were fabricated from thermally grown silicon dioxide. Two mold patterns were defined by electron beam lithography and photolithography, and the molds were etched by RIE with CHF_3 gas. The first mold pattern is a 700nm period grating with 350nm depth. The second mold pattern is a 10 μm period grating with 1 μm depth. The molds were coated with FDTS for anti-sticking and easy mold releasing [38]. Poly (methyl methacrylate) (PMMA) with molecular weight of 15000 (T_g = 105˚C) was used for imprinting and transfer-bonding. Though only PMMA is used to demonstrate the 3D microstructures in this work, other thermoplastic polymers are equally suitable for the techniques developed here. The overall fabrication steps involve cyclic combinations of nanoimprint and transfer-bonding to build up 3D microstructures layer-by-layer as outlined in. First, PMMA is spin-coated on a substrate and the first layer of the microstructure is created by conventional nanoimprint lithography (Figure 14 (a)). The imprint temperature is 175^{o}C and the imprint pressure is 5×10^{6} Pa. The imprint time is 5 minutes. The second PMMA layer should be added to the first PMMA layer by a transfer-bonding technique (Figure 14(c)). For this to work, a PMMA thin film must be placed on top of the mold surface. The PMMA thin film to be transferred to the mold surface is first spin-coated on a substrate that is coated with octadodecyltrichlorosilane (OTS), which makes the surface of the substrate less hydrophobic than that of the mold to avoid dewetting by the PMMA solution. After nanoimprint under the same condition as step 1, demolding is done by twisting the mold against the substrate to ensure that the

PMMA film detaches from the substrate and stays on the mold as shown in Figure 14(b). The PMMA layer on the mold is then transfer-bonded with the first PMMA layer as shown in Figure 14(c). More layers can be added by repeating step 2 and step 3 to construct multilayered polymer microstructures (Figure 14(d)).

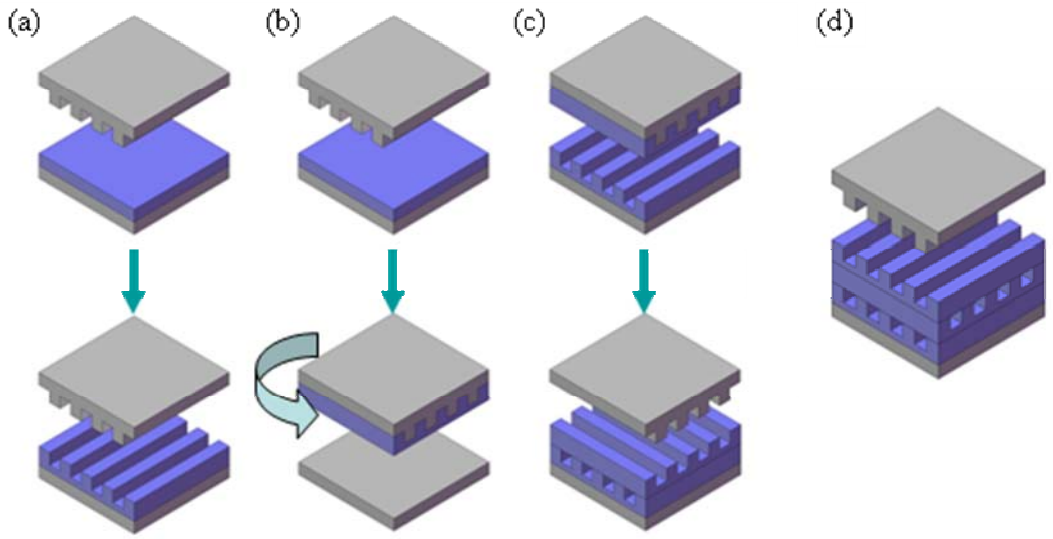

Figure 14. Schematic of the patterning process for 3D multilayer polymer structures. a) Step 1: conventional nanoimprint lithography; b) Step 2: layer transfer from the OTS coated substrate to the mold using twist-demolding; c) Step 3: transfer-bonding; d) Step 4: adding more polymer layers by repeating step 2 and step 3.

2.3 Results and discussion

The two most critical steps in 3D multilayer polymer microstructure fabrication are the layer-transfer of the polymer thin film from the substrate to the mold and the transfer-bonding of the two polymer layers. Both steps need to have a

high yield for the successful fabrication of the multilayered structures. The key factors that affect the yield of these steps and the limitations of past attempts are discussed, and novel methods are developed to address these limitations to achieve 3D polymer multilayer microstructures with high yield.

2.3.1 Reversal nanoimprint

Many variations of nanoimprint have been developed in the last decade to expand the application range of the conventional nanoimprint technique. Reversal nanoimprint is one of such techniques [39-42]. In reversal nanoimprint, the resist film is coated on top of the mold and then transfer-bonded to a substrate. However, placing a polymer film on top of a surfactant-coated mold is not a trivial task because conventional techniques such as spin-coating are seldom successful. Because the mold surface is typically coated with surfactant FDTS, which leaves the mold surface with very low surface energy. Most polymer solvents have a surface energy greater than the critical surface energy of FDTS coated surface so that polymer solutions dewet and bead up on mold surface instead of spreading into a liquid film. When spinning starts, the polymer solution just roll off the mold surface and no polymer film can be coated on mold surface. In order to overcome this issue, several techniques can be used. The first one is to choose a surfactant and solvent combination such that the dewetting of polymer solution on mold surface can be prevented. The second method is to use highly viscous polymer solution because high viscosity can slow down the rate of dewetting and make it possible to leave a film on mold surface after spin-coating.

Finally, it is possible to transfer the polymer film onto the mold surface in a normal thermal imprinting process by treating the substrate with a surfactant such as OTS. OTS and other intermediate surface energy coating (20-40 dyn/cm) can reduce the adhesion between the polymer film and the substrate and also allow many solvents to be used for spin-coating a polymer film on a substrate. Although the mold surface is coated with FDTS (12 dyn/cm), the larger mold-polymer interface due to mold surface patterns can still yield greater mold-polymer adhesion than the polymer-substrate adhesion, which allows the polymer film to be detached from the substrate and remain on mold surface after nanoimprint. To place the polymer thin film on the mold surface, demolding was done by twisting the mold against the substrate as shown in Figure 15. The surfactant coating on the substrate also helps in this step by reducing polymer adhesion to the substrate, thus requiring a small force for twist-demolding. Compared to a direct spin-coating technique, the new method promises very good pattern formation in polymer thin film and achieves a very high yield for layer-transfer.

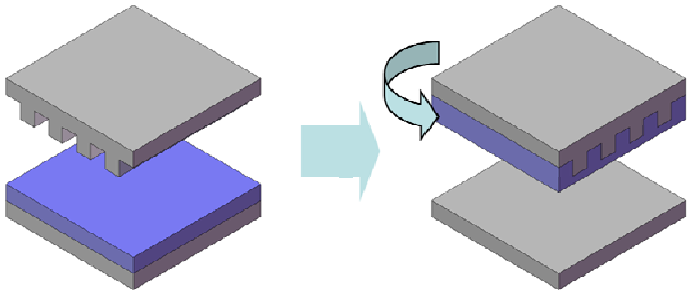

Figure 15. A schematic of transferring polymer film onto mold surface for reversal nanoimprint by twist-demolding in nanoimprint.

2.3.2 Polymer bonding by thin adhesive layer

The critical issue for 3D polymer structure fabrication is the adhesion between the polymer layers. In order to successfully transfer the polymer layer from the mold to an existent polymer layer on the substrate, the adhesion between the polymer layers must be greater than the adhesion between the mold and the polymer. This is difficult to achieve for most polymer materials, particularly thermoplastic polymers. One straight forward method to solve this problem is by using a thin adhesive layer, such as SU-8, to bond the two polymer surfaces. The schematic of using a thin adhesive layer is shown in Figure 16 (a). SU-8 was purchased from Microchem and diluted in propylene glycol methyl ether acetate (PGMEA) to form 1 wt. % to 10 wt. % solutions. By quickly spin-coating diluted SU-8 solution on the top of the PMMA thin film on the mold surface, a very thin layer of SU-8 layer (~10 nm) can be deposited while dissolving of the PMMA thin film is minimal. The transfer bonding process was done at 80^{o}C. Since the glass transition temperature of SU-8 is 64˚C [43], the melted SU-8 allows a good interfacial layer to be formed to enhance adhesion, while the PMMA layer still remains in solid form because of the low bonding temperature. UV-curing of SU-8 after bonding was not necessary and actually not done. Multilayer structures in PMMA can be easily obtained with high yield as shown in Figure 16 (b).

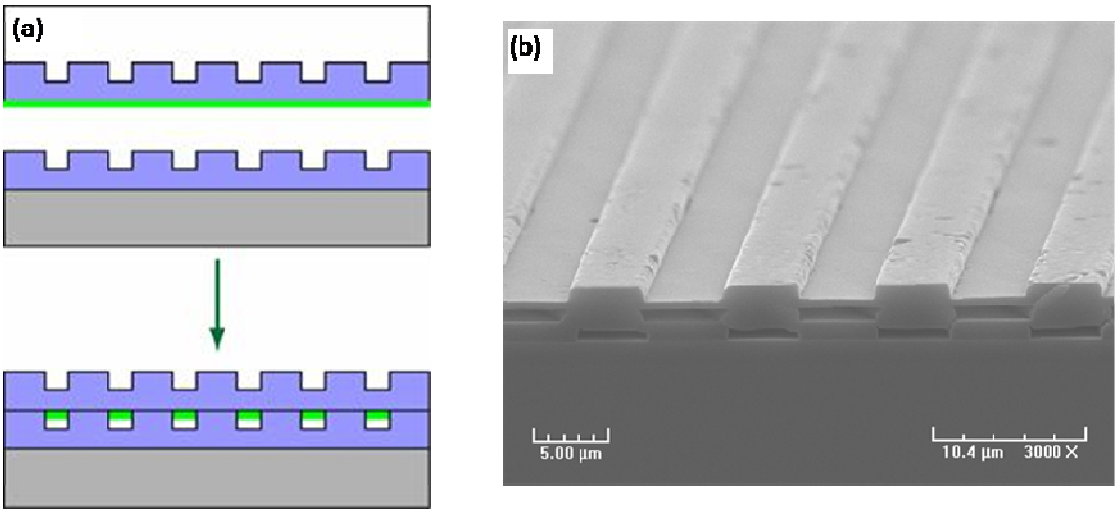

Figure 16. (a) Schematic of fabricating multilayer polymer structures by bonding with a thin adhesive layer; (b) Three-layer PMMA microstructure bonded by a thin SU-8 adhesive layer.

There are several advantages of using thin adhesive layers. The SU-8 "glue layer" is very thin so that the overall PMMA structure can still be easily removed by solvents, unlike the 3D polymer structures based on UV-cured thermoset polymers. This bonding method has very high yield, approaching to nearly 100%. Another significant advantage is that this technique is non-specific, which means it is suitable for any polymer and inorganic material, thus opening up the possibility of creating hybrid composite structures by combining different materials.

The disadvantage of using thin adhesive layers is that the thickness of the SU-8 layer must be carefully controlled. Excess SU-8 will partially or completely fill the bottom layer patterns. As shown in Figure 17, as the thickness of the SU-8 layer increases, more bottom layer structures are filled. For 1 wt. % SU-8, 350 nm structures

can be clearly seen; while for 10 wt. % SU-8, no bottom layer structures can be seen in the SEM micrographs, which indicate that all bottom layer structures were filled by SU-8. Using thin adhesive layer can introduce another issue. For some applications, such as 3D multilayer structures in functional polymers, the introduction of SU-8 can be problematic because alien SU-8 can interfere with the functional materials. Ideally a technique that can achieve 3D multilayer microstructures in a single thermoplastic polymer is desired.

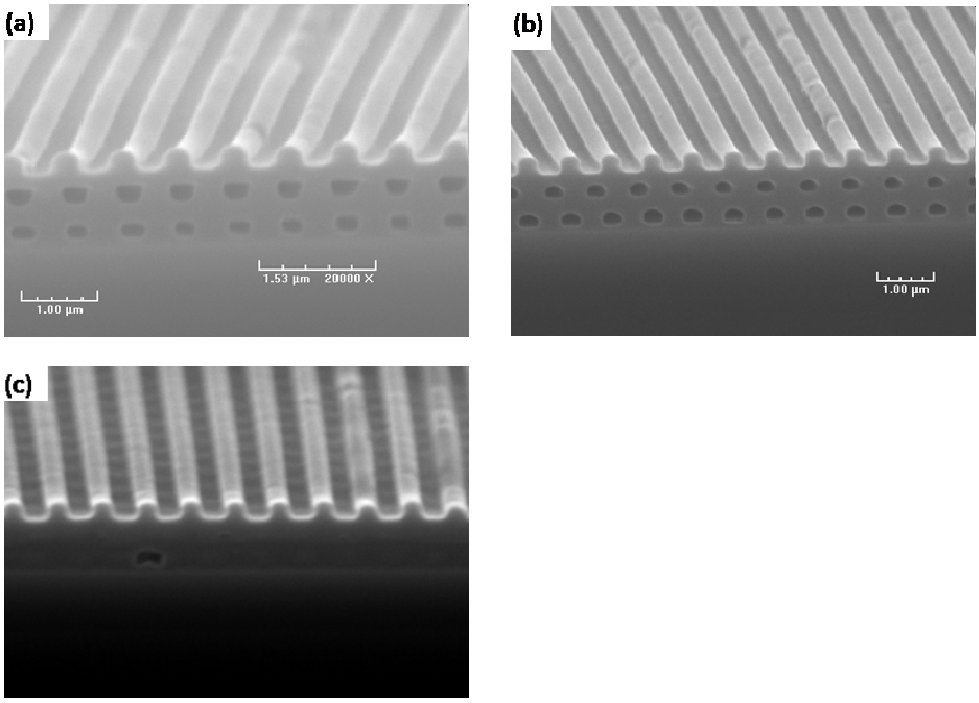

Figure 17. SEM micrographs of 3D multilayer PMMA structures using SU-8. (a) Three-layered 700 nm pitch grating bonded with 1% of SU-8; (b) Three-layered 700 nm pitch grating bonded with 6% of SU-8; (c) Three-layered 700 nm pitch grating bonded with 10% of SU-8. Progressively more bottom layer structures filling is observed from (a) to (c).

2.3.3 Direct thermal bonding near T_g

Multilayer polymer microstructures in a single thermoplastic polymer can be achieved by direct thermal bonding. However, the processing conditions (temperature and pressure) must be carefully determined. If the bonding temperature is much lower than the T_g of the polymer in order to preserve the bottom polymer structure, the adhesion between the two polymer layers is very week, and bonding will most likely fail. If the bonding temperature is well above the T_g of the polymer, though good adhesion can be achieved between the polymer layers due to interfacial mixing, the bottom polymer structure will be severely deformed, leading to failure of the multilayer structure.

To avoid this dilemma, direct thermal bonding of thermoplastic layers was performed at a temperature slightly below the T_g of the polymer. This scheme takes advantage of the fact that the polymer T_g in the surface region and therefore polymer mobility is usually 5-10^{o}C lower than that of the bulk polymer [44, 45]. To ensure good adhesion between two polymer layers, only 2-3 nm of interfacial mixing is enough. Bonding at a temperature slightly below the bulk T_g allows the formation of a good interfacial mixing layer due to surface mobility, while the bulk of the bottom polymer layer is still below T_g to preserve pattern integrity.

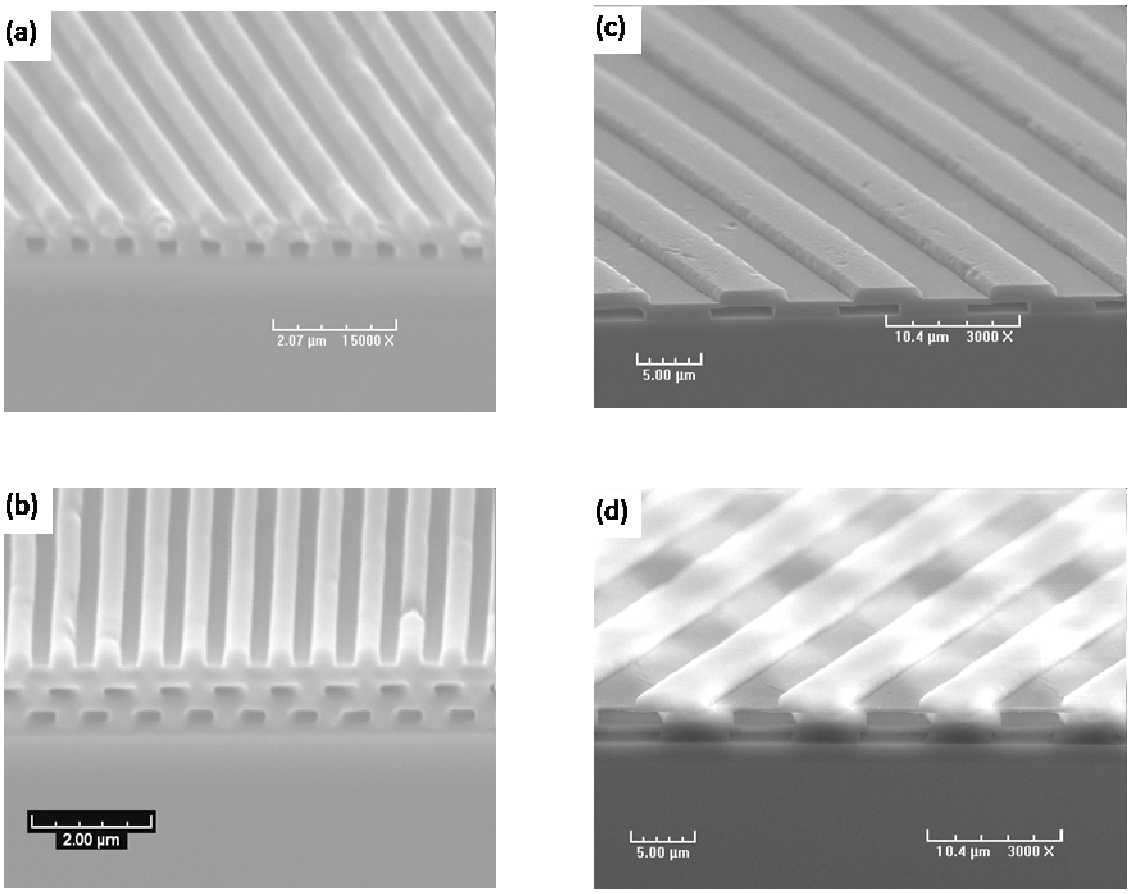

Figure 18. SEM micrographs of 3D multilayer PMMA structures using direct thermal bonding. (a) Two-layered 700 nm period grating; (b) Three-layered 700 nm period grating; (c) Two-layered 10 μm period grating; (d) Three-layered 10 μm period.

Successful fabrication of multilayer microstructures in PMMA was achieved by performing the bonding at 100^{o}C. The bonding pressure used is 3×10^{6} Pa. Multilayer structures of different sizes are shown in Figure 18. Two-layer and three-layer submicron gratings are shown in Figure 17(a) and (b), and two-layer and three-layer gratings of 10 μm are shown in Figure 17(c) and (d). Though PMMA is used in

these multilayer structures, this method is equally applicable to other thermoplastic polymers including many functional polymers, thus providing freedom in material choice when creating 3D multilayer microstructures for specific applications.

2.3.4 Solvent damping method

Solvent damping can also be used for multilayer bonding. The bonding condition is same as direct thermal bonding method at a bonding temperature of 100^{o}C and a bonding pressure of 3×10^{6} Pa.. In this case, PGMEA was spin-coated on top of the polymer layer on the mold just before transfer bonding, similar to the case where SU-8 was used as thin adhesive layer in previous method as shown in Figure 16(a). The advantage of this method is that it can take the advantage of both bonding with thin adhesive layer and direct thermal bonding. The spin-coated PGMEA quickly introduces a thin soft layer on top of the bulk to improve the adhesion like SU-8. PGMEA also does not affect polymer functionality, unlike the SU-8. Figure 19 show the SEM image of multilayer of PMMA structure fabricated by solvent damping method. Left picture shows the two layers of 700nm gratings and right picture shows two layers of 10 μm gratings. In the experiment, the yield is slightly higher than direct thermal bonding but lower than bonding with thin adhesive layer.

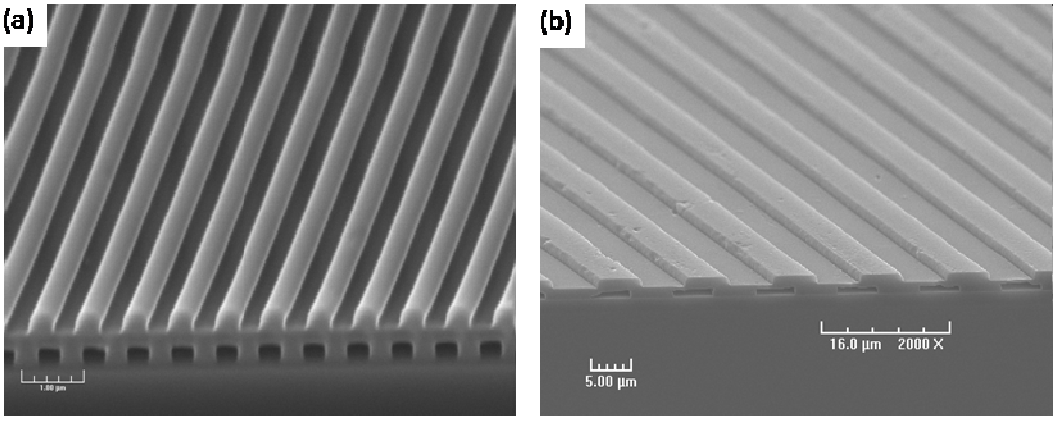

Figure 19. SEM images of 3D multilayer PMMA structures using solvent damping. (a) Two-layered 700 nm period grating and (b) two-layered 10 μm period grating.

2.3.5 Factors affecting process yield

For a fabrication technique to be practically useful, it must have good process yield. In building polymer 3D structures by reversal nanoimprint and transfer-bonding, the most important issue is the competition between the mold-polymer adhesion and the polymer-polymer adhesion. The mold-polymer adhesion depends on the type and the quality of the mold surfactant coating, the compatibility of the polymer and the surfactant, and the pattern depth and density. The total mold-polymer interfacial area, thus adhesion force, will increase with increasing mold pattern depth and density as shown in Figure 20. Consequently, it is more difficult to transfer-bond high-density and high aspect-ratio nanostructures. For finer patterns, the increased sidewall interfacial contact between mold and polymer greatly enhances mold-polymer adhesion, thus making it more difficult to achieve high yield. The pattern in each

polymer layer also has an impact on process yield. When transfer-bonding a polymer layer onto a bottom polymer grating instead of a uniform polymer film, the total contact area between the two polymer layers become much smaller. For higher process yield, it is preferred to have a larger ratio of the protrusion area to the recessed area in the bottom polymer layer.

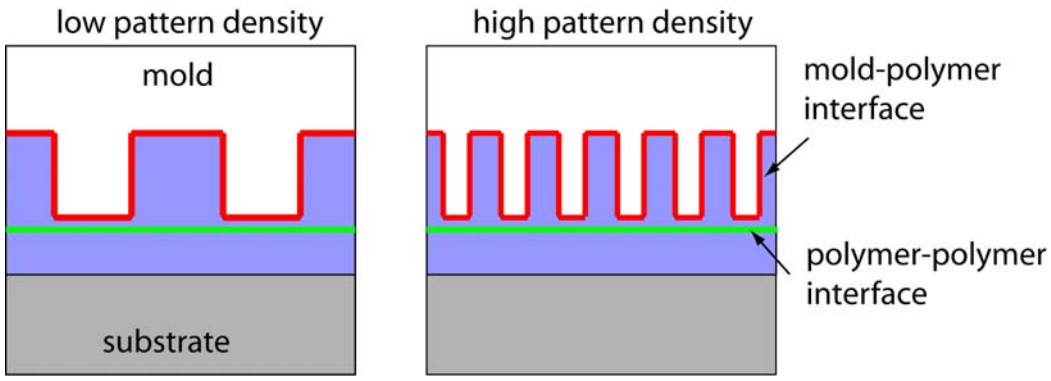

Figure 20. Larger mold-polymer adhesion for mold patterns of higher density.

The polymer-polymer adhesion is an even more complicated issue and itself is a subject of intensive research with significant industrial impact [46, 47]. In general, polymer-polymer adhesion strongly depends on the nature of the polymers and their interfacial interactions. For different polymer materials, interfacial interactions can be categorized into several types: van der Waals force, hydrogen bond, electrostatic attraction and covalent chemical bonds. Strong interactions, such as covalent bonding, can lead to excellent polymer bonding. Very high transfer-bonding yield can be achieved because the polymer-polymer adhesion is much greater than the mold-polymer adhesion. The opposite is true for weak interfacial interactions, such as van

der Waals force, which often leads to failed transfer-bonding. Chemical bonding can usually form at polymer interface if the polymers are briefly treated by oxygen plasma before bonding. Forming intermixed layers at the interface by heating the polymers to near their T_g can also greatly enhance polymer-polymer adhesion. Finally, the mechanical strength, which is the magnitude of the cohesive force that holds the polymer chains together, also has an impact on the transfer-bonding yield. If both mold-polymer and polymer-polymer adhesion forces are greater than the mechanical strength of the polymer materials, it is inevitable that the polymer layer will be torn off – part of the polymer layer is transferred to the substrate and but the rest remains on mold. This may become a significant issue when bonding very thin polymer layers because of their weak mechanical strength. Due to the complexity of adhesion forces, typically it requires a case by case study to improve process yield based on the polymer materials used and the details of the patterns in each layer.

The overall yield of fabricating 3D multilayer structures is determined by the process yield of each step in . For nanoimprint and layer-transfer, close to 100% yield can be achieved by careful surfactant treatment on mold and substrate and by twist-demolding. The yield-limiting step is thus the transfer-bonding of a new polymer layer to an existent polymer multilayer structure. The yield of different transfer-bonding schemes is shown in . In all bonding schemes, particles are found to be the major limiting factor in achieving high process yield because they prevent conformal contact of the two polymer layers to be bonded. As shown in , the transfer-bonding yield is also found to be dependent on the pattern size itself when particles are carefully

avoided in the experiments. Larger patterns (10 μm period grating) feature higher bonding yield than finer patterns (700 nm period grating). In the situation where an adhesive layer, such as a thin SU-8 film, can be used, the process yield of transfer bonding can be very high. Larger patterns (10 μm period grating) has higher bonding yield compared with finer patterns (700 nm period grating). For finer patterns, the increased sidewall interfacial contact between the mold and the polymer greatly enhances the mold-polymer adhesion, thus making it more difficult to achieve high yield.

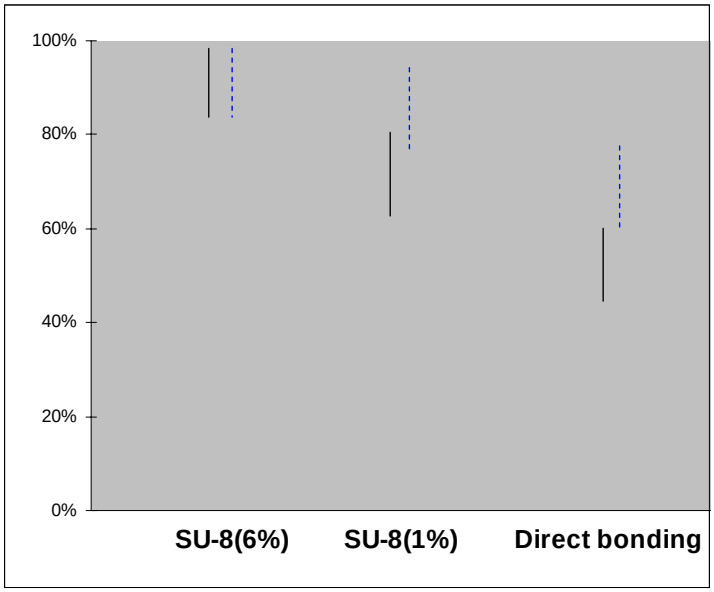

Figure 21. Yield of 3D PMMA structures with different bonding schemes for different patterns: 10 μm period grating (dashed line) and 700 nm period grating (solid line).

Though the yield for direct thermal bonding is lower in this study, it is expected that further optimization of processing conditions such as fine-tuning the bonding temperature and pressure can improve the yield to a level high enough for practical applications. Coupled with the flexibility in material and pattern choices for each polymer layer, the decent to high process yield enables simple yet efficient fabrication of 3D multilayer polymer microstructures, thus opens up many novel applications based on 3D multilayer structures.

2.4 Summary

In this project, we developed and optimized techniques which enable us to fabricate 3D multilayer polymer microstructures. The optimized layer-transfer and transfer-bonding techniques promise high yield, high throughput and good polymer pattern formation. For layer-transfer, twist-demolding ensures good polymer placement on the mold surface for subsequent transfer-bonding. Bonding with a thin adhesive layer and direct thermal bonding near T_g were experimented for polymer transfer-bonding with high yield. Aside from achieving near 100% yield, the thin adhesive layer can also be used to bond heterogeneous materials, such as two different polymers or polymer and inorganic materials, thus making it an ideal method for creating 3D structures based on polymer-inorganic composite materials. The thickness of the adhesion layer needs to be precisely controlled to avoid filling of the bottom layer patterns. The direct thermal bonding near T_g is a generic method that is suitable for all thermoplastic materials, making it extremely versatile in combining different

polymer materials for novel applications. By using a different material or a different pattern in each layer, the multilayer fabrication methods developed in this work allow almost unlimited combination of scenarios, thus provide great flexibility in designing and fabricating 3D multilayer structures with unlimited layers for a broad range of applications. The process yield of multilayer structure fabrication is affected by the existence of particles and the density and sizes of the mold patterns. Upon further improvement of process yield, it is believed that the optimized fabrication methods will spur the application of multilayer structures in electronics, photonics and bioengineering.

CHAPTER III

THERMOPLASTIC POLYMER PATTERNING WITHOUT RESIDUAL LAYER BY ADVANCED NANOIMPRINT SCHEME

3.1 Introduction

As a mentioned earlier, nanoimprint lithography is considered as one of the candidates for next generation lithography techniques for future microelectronic fabrication. Aside from the lithography application, another advantage of nanoimprint is its ability to directly create micro- and nanostructures in functional polymers such as semiconducting [48-51] and piezoelectric polymers [52, 53]. This is because thermal nanoimprint only needs temperature and pressure for pattern replication, which both are benign to functional polymers. This feature opens up the possibilities in nondestructive patterning of functional polymers at the micro- and nanoscale for novel applications in electronics, optoelectronics, photonics, sensors and bioengineering.

Although NIL technique is developing rapidly in recent years, there are still issues that need to be addressed for broader adoption of the nanoimprint technique. One of the problems is the residual layer that remains in the polymer pattern after nanoimprint. Conventional approach to remove the residual layer is to use an oxygen RIE process [34]. Nanoimprint is a fast process that can be accomplished within a few minutes, which is critical for high throughput fabrication of nanostructures. The oxygen RIE step involves vacuum processing that can significantly increase the overall processing time and greatly lower nanoimprint throughput. More severely,

oxygen RIE can degrade or even damage the functional polymers by breaking the polymer chains with highly energetic oxygen ions. This eliminates the possibility to create isolated functional polymer structures by nanoimprint for device and system applications, particularly in integrated microsystems where good isolations between devices are needed. Another method to avoid the residual layer is to use the combined-nanoimprint-and-photolithography technique [54]. However, this technique is only suitable for UV-curable polymers, not most functional polymers which are thermoplastic. It is thus highly desirable to develop a new technique to remove the residual layers without RIE for thermoplastic polymers. In order to further lower the cost and enhance the throughput of nanoimprint, and extend nanoimprint to patterning isolated functional polymer micro- and nanostructures, new residual layer removal techniques need to be developed.

In a conventional thermal nanoimprint, the residual layer is located at the bottom of the patterned polymer thin film. It is thus not possible to access the residue layer without affecting the polymer patterns. To circumvent this problem, we first transfer the polymer thin film from a flat substrate to the nanoimprint mold, thus exposing the residual layer to the outmost while the polymer structures are preserved inside the trenches of the mold. This allows the residual layer to be easily removed by nondestructive means. After residual layer removal, the functional polymer pattern can be transferred to a substrate by a reversal nanoimprint [39] or a transfer-bonding [55] process. The final structures on the substrate are polymer micro- or nanostructures without residual layer.

This 3D multilayer structure, having no residual layer, can be used for unique applications such as templates for advanced inorganic 3D structure. Because inorganic 3D structure is very difficult to fabricate in current techniques and also materials are very limited, the application is very limited in microelectronics, although it has great advantages of certain applications. The limitation to create 3D inorganic structure can be easily solved with newly developed method. The demonstration of creating 3D inorganic structure using electroplating is shown in this chapter.

3.2 Techniques to remove residual layer

In this work, two methods are used to remove the exposed residual layers. The first method is a solvent developing technique. The functional polymer on a nanoimprint mold is soaked in a container with solvents. The outmost residual layer is gradually dissolved and removed from the mold surface, and the complete removal of the residual layer can be achieved by controlling the developing time based on the dissolution rate of the polymer material. The second method utilizes the dewetting of a thin polymer film on an incompatible surface. By carefully controlling the residual layer thickness and annealing temperature, residual layers on top of the mold protrusions can be cleared and get collected in mold trenches. Both techniques presented here do not affect the chemistry of the polymer materials. They are suitable for all thermoplastic polymers, including functional polymers.

The 700 nm period grating mold with 350 nm depth and 10 μm period grating mold with 0.8 μm depth for nanoimprint was fabricated in 1.0 μm thick thermal oxide

on silicon substrate. The patterns are defined by electron-beam lithography and photolithography for 700 nm and 10 μm period gratings respectively. The grating structure is etched into the thermal oxide layer by RIE with CHF_3 gas. The molds were coated with FDTS to render the mold surface hydrophobic for easy mold releasing. The low surface energy is also needed for the dewetting process to occur. The molds were cleaned by piranha solution (sulfuric acid: 30% hydrogen peroxide = 3:1) for 30 minutes before FDTS coating. The coating was done by soaking the molds in heptane with a few drops of FDTS for 10 minutes.

All polymer films (15k and 75k PMMA, MEH-PPV and P3HT) are prepared from spin-coating of polymer solutions. To reduce polymer-substrate adhesion for easy transfer of polymer film onto mold surface after nanoimprint, the silicon substrates were first coated with OTS. The OTS coating procedure is the same as that of FDTS. Soft bake was done at 95°C for 2 minutes on hotplate to remove solvent in films after spin-coating. For the layer-transfer, the polymer film on the substrate was imprinted at 175°C for 5 minutes with 5×10^6 Pa and then this pressure was maintained until the temperature falls to room temperature. After releasing pressure, polymer layer was transferred to the mold by slight twisting of mold against substrate. Unlike conventional vertical separation of the mold and substrate assembly, the polymer film was detached from substrate and attached on mold surface.

3.2.1 Solvent developing

The first method to remove the residual layer is to dissolve polymer residues on the mold with organic solvents such as PGMEA or toluene. Several polymers were chosen to prove the feasibility of this approach: 1) PMMA with average molecular weights of 15k and 75k; 2) poly(3-hexylthiophene) (P3HT) and poly[2-methoxy-5-(2'-ethylhexyloxy)-1,4-(1-cyanovinylene)phenylene] (MEH-CN-PPV), both are polymer semiconductors that are widely used in organic electronics such as thin-film transistors, light-emitting diodes and photovoltaic devices. The polymer was spin-coated on a silicon substrate that is treated with OTS to reduce polymer-substrate adhesion and then imprinted with grating molds that were coated with FDTS. All nanoimprints were done at 175°C and 5×10^6 Pa. After nanoimprint, the mold and the substrate were separated by twist-demolding [56], which results in the detachment of the polymer film from the substrate. For flexible substrate or mold, transferring a polymer film to a mold surface may also be done by controlled peeling [57, 58]. The mold, along with the polymer film, is then immersed into a solvent for the residual layer removal at room temperature for a fixed amount of time. After a target thickness of polymer film is removed, the mold was placed into a spin-coater and dried by spinning and soft baking (Figure 22(b)). Since the mold surface has very low energy, solvent does not cling to the mold protrusions and the residual layer can be completely removed. To find out the dissolution rate of polymer films in common solvents, we also spin-coated polymer films on a flat silicon surface. The dissolution rate can be calculated based on the film thickness measurement by ellipsometer and profilometer after fixed soaking

time. Figure 23 shows that the dissolution rates for several polymers in different solvents. The overall dissolution rate of 75k mw PMMA is around 3nm/s in both PGMEA and toluene. The dissolving speed is faster at the beginning and slows down as dissolution progresses. Compared to 75k mw PMMA, 15k mw PMMA has a much faster removal rate in both solvents due to shorter chain length. The etching rate of MEH-PPV in toluene is around 2nm/s. However, the dissolution rate shows some variation for MEH-PPV in various tests. The variation may be contributed to internal polymer chain morphology difference in those films.

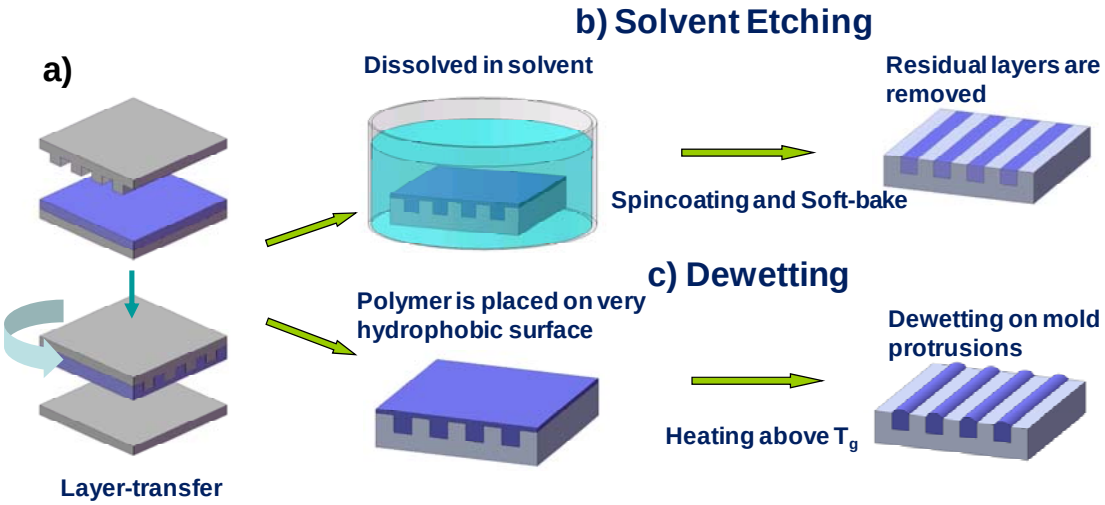

Figure 22. Schematic of a) layer-transfer method to place polymer film on mold surface; b) solvent developing method and c) dewetting method for residual layer removal.

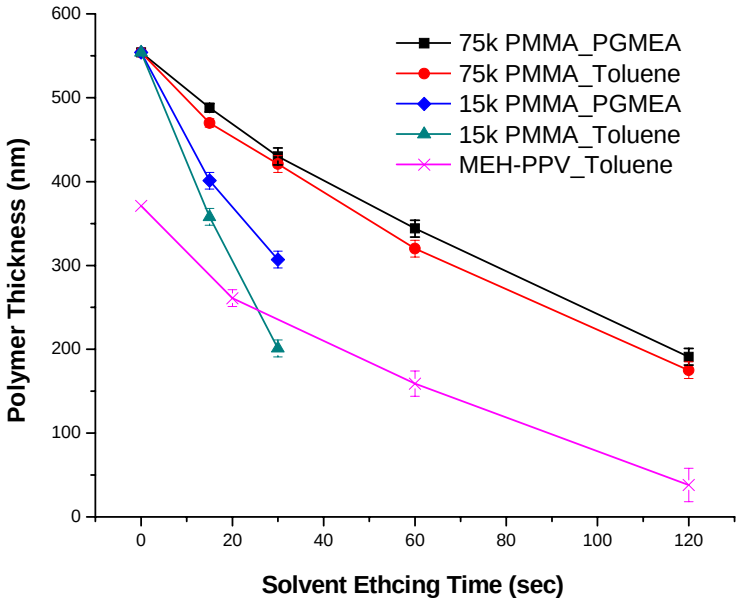

Figure 23. Polymer dissolution rates in solvents.

After complete removal of residual layers by controlling the dissolving time based on the removal rate and residual layer thickness, the polymer films are then transferred onto substrates with the transfer-bonding technique. Figure 24 shows the fluorescent microscope images of patterned functional polymers on a polymer or a bare silicon substrate under UV illumination. The MEH-PPV microstructures on a polymer substrate with and without residual layers are shown in figure 24 (a) and (b), respectively. A similar pattern without residual layer on a Si wafer is shown in figure 24(c). Due to the presence of the residual layer, red fluorescence from MEH-PPV is observed throughout the film. The dark regions in Figure 24(b) and (c) indicate complete removal of the residual layers, and isolated MEH-PPV patterns of around 10 microns are achieved with well-defined geometry. Figure 24(d) shows the P3HT

patterns without residual layers on a polymer substrate. Coupled with nanoimprint's high resolution, solvent developing and transfer bonding will allow us to directly create isolated fine patterns of functional polymers, which cannot be achieved by other patterning techniques such as ink-jet printing in which patterns are limited to tens of microns and larger due to liquid spreading [51, 59].

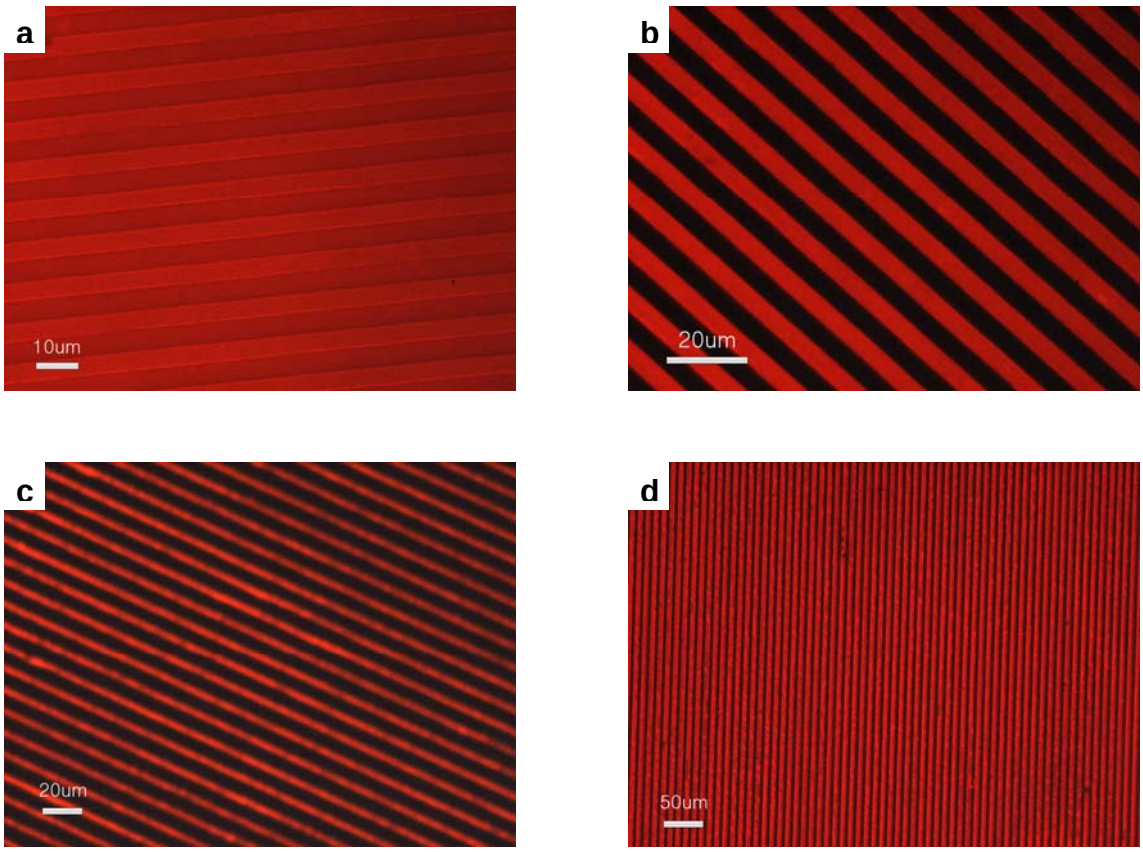

Figure 24. Fluorescence microscope images of patterned functional polymers. a) MEH-PPV with residual layer on PMMA, b) MEH-PPV without residual layer on PMMA, c) MEH-PPV without residual layer on Si, and d) P3HT without residual layer on PMMA.

3.2.2 Principle of dewetting

The second method to remove the residual layer without RIE is through controlled dewetting. Dewetting is the spontaneous withdrawal of a liquid film from an incompatible surface. An understanding of the thin polymeric film on solid substrate such as wetting and dewetting process is considerably important in many applications so that it has been studied for many years. An understanding of the thin polymeric film on solid substrate such as wetting and dewetting process is considerably important in many applications so that it has been studied for many years [60-65]. It is shown that the final polymer morphology of a dewetting process depends on many factors, such as the thickness and viscosity of the polymer melt, the interfacial interaction between the polymer melt and the substrate, the shape and size of the topographical and chemical patterns on the substrate, and growth kinetics. When the polymer is relatively thick (>100 nm), the van der Waals force is weak. However, when the polymer film is thin enough (<100 nm) the van der Waals force becomes dominant force and the film is placed in unstable condition. Dewetting is the one of the phenomena that occurs at the interface between a liquid-solid and liquid-liquid substrate. Generally, dewetting describes the rupture of a thin liquid film on the substrate shown in Figure 25 and formation of droplets. To have a dewetting process, some of important preconditions should be required in spreading coefficient, film thickness and surrounding temperature. First of all, the negative spreading coefficient is needed, which is defined with this equation,

$$S=\gamma_s - (\gamma_{sp} + \gamma_p),$$

where γ_s is the surface energy of the substrate, γ_{sp} is the interfacial energy between the polymer film and the substrate and γ_p is the surface energy of the polymer film. When the S is positive, the surface is considered wettable. For example, surface energy of the substrate is high enough for spreading coefficient to be positive. When the surface energy of substrate becomes decreasing due to surfactant coating, the spreading coefficient becomes negative, and then the polymer film can start to dewet. Although the spreading coefficient is negative, the polymer film does not start to dewet immediately. In case when the polymer film is very thin (~100 nm) and the ambient temperature is above its glass transition temperature (T_g), the mobility of polymer chain molecules is increasing and thin polymer film is undergoing dewetting with spontaneous nucleation and spinodal decomposition.

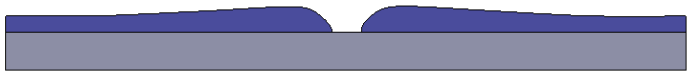

Figure 25. The rupture of thin liquid film on substrate.

Figure 26 shows the progress of dewetting process. First of all, the polymer film is breaking up thus creating randomly distributed holes. And then these holes continually grow and the rims of the holes merge each other. From this merging process, the isolated droplets are generated. In the dewetting process, the number of droplets is inversely proportional to thickness of polymer and the diameter of droplets is proportional to the thickness of polymer. The reason is that the average distance

between initial holes are proportional to square of film thickness. So in thin polymer case, there are lots of holes and then after merging process the small size of droplets and lot of isolated droplets are generated.

$$N_{Droplet} \propto \frac{1}{T_{Polymer}}$$

$$D_{Droplet} \propto T_{Polymer}$$

$$\text{Average distance between initial holes } \sim T_{Polymer}^{2}$$

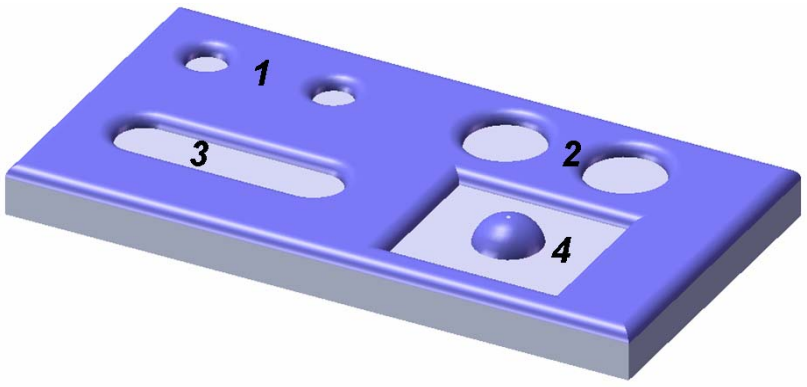

Figure 26. The progress of dewetting process. 1) randomly distributed holes, 2) continually grow, 3) the rims of the holes merge each other and 4) from this merging process, the isolated droplets are generated.

But for the thick polymer case, there are fewer number of holes and then after merging process the larger diameter of and smaller number of isolated droplets are generated. But thick polymer case, there are small number of holes can be generated. The diameter of droplet is proportional to thickness of polymer but number of droplets

is inversely proportional to film thickness. So the Thickness is the most important role for dewetting process.

3.2.3 Dewetting on mold to remove residual layers

After placing the polymer thin film on top of the surfactant-coated mold surface, heating the mold to a temperature above the glass transition temperature (T_g) of the polymer can induce automatic dewetting because the residual polymer layer, which is usually thinner than 100 nm, is located on top of the low-energy mold protrusions. The residual layer will start to rupture due to spontaneous nucleation and spinodal decomposition, and the residual polymer will be gradually removed from mold protrusions to mold trenches as the pinholes grow (Figure 22(c)).

Though most dewetting patterns on a homogeneous surface are random holes or droplets arranged in polygonal pattern, long-range order can be achieved on topographically [66, 67] or chemically [68, 69] patterned substrates. For clearing the residual polymers on mold protrusions, the ideal result is to achieve a long-range order such that dry region occupies the whole protrusion area and all residual polymers are collected at mold trenches. This can be achieved by control the dewetting temperature and the residual layer thickness based on the size and shape of the protrusions. We have experimented with several combinations of residual layer thickness and mold protrusion sizes. The final morphologies of the polymer materials after dewetting in these situations are shown in Figure 27.

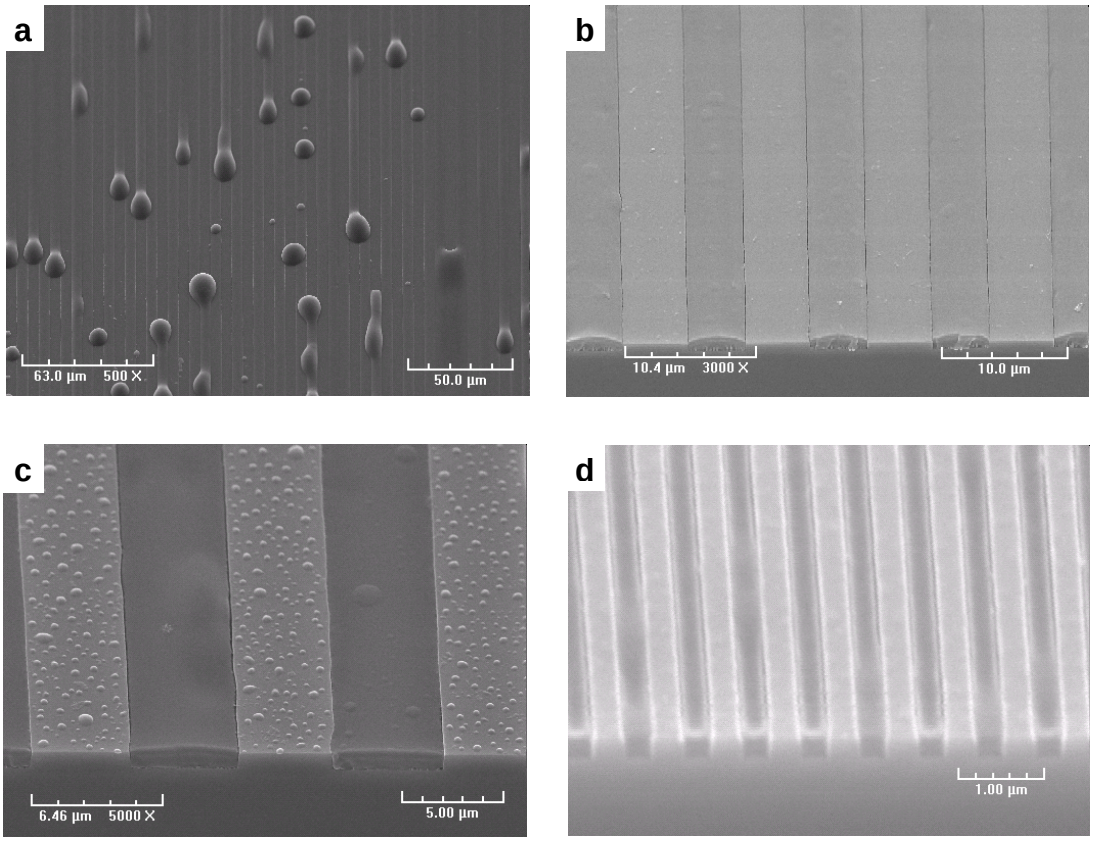

Figure 27. SEM micrographs of PMMA structures on the mold after dewetting process in case of (a) Thick residual layer (>200nm), scale bar 50 m; (b) Medium thickness of residual layer (~100 nm), scale bar 10 μm; (c) Very thin residue layer (<20 nm), scale bar 5 μm; (d) 350nm gratings after dewetting, scale bar 1 μm.

Since PMMA can dewet on a hydrophobic surface such as FDTS-coated mold surface, PMMA of various thicknesses are transferred onto the mold with layer-transfer method as described in Figure 22(a) to test dewetting morphology. When the residual PMMA thickness is very thick (> 200 nm), no dewetting is observed. When the residual layer thickness is less than 200nm, dewetting produces overspilling

droplets [66] or bulges [70] that are centered at mold trenches and spread over neighboring mold protrusions, as shown Figure 27(a). Figure 27(b) shows the mold after dewetting with around 100nm residual layer. Initial holes formed due to spinodal dewetting grow and the liquid front lines withdraw to the edges of the protrusions. As a result, the polymer on the protrusions is completely moved to the trenches to form extended filaments [66] that have a convex meniscus due to positive Laplace pressure. For very thin residual layer, such as ~ 20nm thick, the final dewetting morphology is scattered small droplets on mold protrusions, as shown in Figure 27(c). Since the average distance between initial holes in spinodal dewetting is proportional to the square of film thickness, closely packed holes are formed in a very thin polymer film. Those holes touch each other and the boundary lines quickly decompose into small droplets that are separated from the liquid front lines and left on the protrusion area. In this situation, residual polymers are just reorganized on mold protrusions.

The final distribution of the residual polymer will be determined by the length scale of the mold patterns and the inherent length scale of the dewetting process, which is related to the polymer film thickness. It is thus possible to achieve regular dewetting pattern for complete residual layer removal by choosing an appropriate residual layer thickness based on the mold protrusion patterns. The residual layer thickness can be easily controlled based on mold depth and initial film thickness. Figure 27(d) shows a 700-nm period grating mold after dewetting, in which the residual layers are completely removed from the protrusions. To further prove the complete removal of the residual layers, the polymer pattern without residual layer can

be transfer-bonded to a substrate and metal liftoff can be performed. Figure 28 shows an optical microscope image of a 10 μm period gold grating obtained after gold evaporation and lift off in acetone, which demonstrates that no residual layer is left in polymer grating.

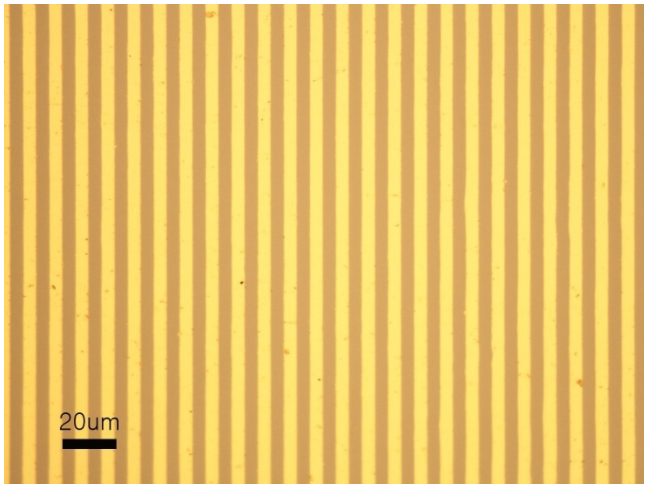

Figure 28. Optical microscope image of 10 μm period gratings after lift-off.

In previous chapter, we optimized transfer-bonding technique for the fabrication of three-dimensional (3D) microstructures based on thermoplastic polymers such as PMMA [71]. Due to the residual polymers, the multilayer structures are not open between neighboring layers. In some applications of 3D polymer microstructures, connectivity between different layers is desired, such as in advanced multilayer fluidic device where fluids need to be transported through different layers. The residual layer removal technique developed here can be easily adopted in the multilayer polymer microstructure fabrication process. The fabrication scheme is

depicted in Figure 29. After removing the residual layer by dewetting or solvent developing, the second layer is transfer-bonded on top of the first layer that was fabricated by a conventional nanoimprint step (Figure 29 (a)). The transfer-bonding was done at 95°C and 3×10^6 Pa for 30 minutes. Repeating the transfer-bonding step can add more layers to the 3D polymer microstructures.

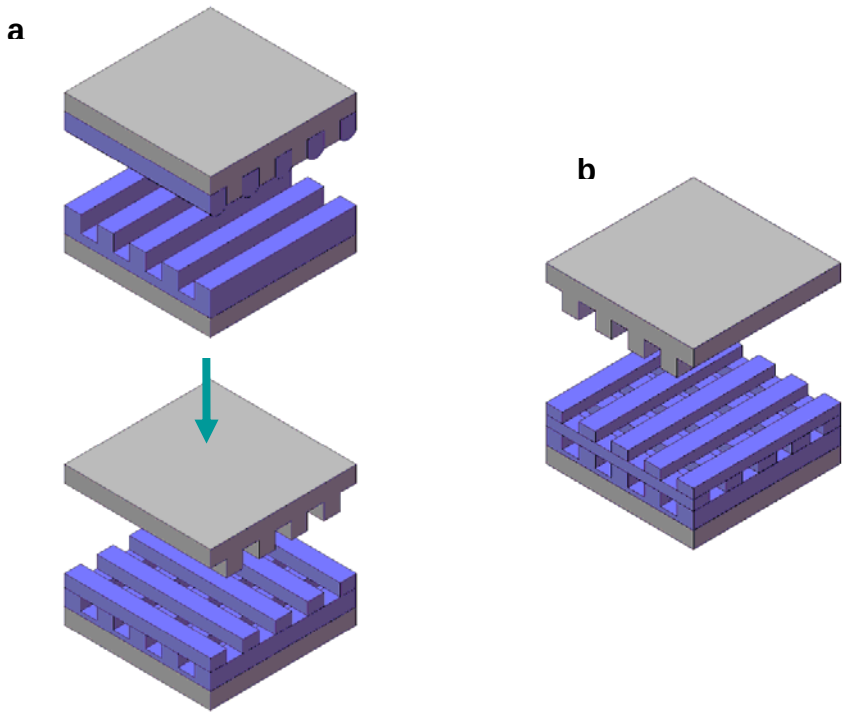

Figure 29. Schematic of 3D polymer patterning process. a) Transfer-bonding a polymer grating without residual layer to another polymer grating and b) adding more polymer layers by repeating transfer-bonding.

Figure 30(a) and (b) shows 3D multilayer structures of PMMA with residual layers removed by dewetting and solvent developing, respectively. Such 3D polymer

structures are expected to find numerous applications such as polymer scaffolds and multilayer microfluidics for bio-MEMS, or serving as sacrificial templates for inorganic 3D microstructures where the thermoplastic polymer templates can be easily removed by solvents.

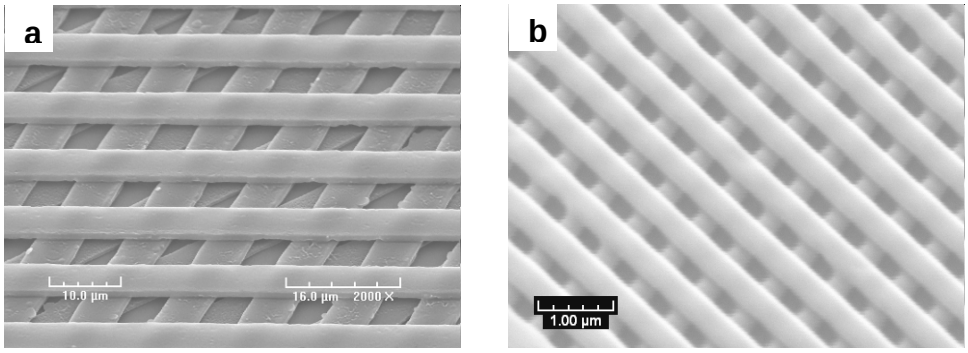

Figure 30. SEM micrographs of 3D multilayer PMMA structures with a) 10 μm period gratings, residues removed by the dewetting method b) 700nm period gratings, residues removed by solvent etching method.

3.3 Templates for advanced inorganic 3D structures

The limitation to create 3D inorganic structure can be easily solved with our newly developed method. Figure 31 shows how to fabricate 3D inorganic multilayer structure. First of all, 3D multilayer polymer structures without residual layers are fabricated. Once the polymer 3D multilayer structures are ready, inorganic materials such as metal, dielectrics or solution processed nanomaterials can be infiltrated inside the polymer structures. Finally, the polymer template is removed with solvent soaking. For these applications, the original template should be fabricated with thermoplastics

polymers, not thermoset polymers, so that the template can be removed by solvent easily.

Figure 31. The process of fabricating 3D inorganic structure with 3D polymer template.

In this work, the nickel electroplating was used for demonstration of such inorganic 3D structure. Electroplating is an electrochemical process that uses electrical current to reduce cations of a desired material from a solution and coat a conductive object with a thin layer of the material, such as a nickel. The nickel sulfamate solution, composed of boric acid, nickel sulfamate and nickel chloride, was prepared for nickel electroplating.The substrate was coated by a thin nickel layer (100 nm) by evaporation to serve as seed layer for electroplating. Then, the multilayer 3D structure with 10 μm gratings (Figure 30(a)) was fabricated on top of this nickel layer. For nickel electroplating, a small piece of high purity nickel (2" diameter nickel square) loaded into solution basket is used as anode. The sample with seed layer is used as cathode was loaded into the solution. The thickness of nickel coating is calculated from the Faraday's law,

$$h = 0.000869*c*J*t$$

where, h is coating thickness (μ inch), c is coefficient of cathode efficiency (about 0.95), J is electric current density (A/ft²) and t is time (min). The total target thickness was 50 μm. Hydrogen bubbles from water electrolysis formed on the cathode surface and adhered to it may cause pitting of the deposit. In order to enhance removal of the bubbles, ultrasonic agitation was used for the whole electroplating process. Figure 32 shows the nickel (Ni) 3D structure which was electroplated from 3D polymer structure as explained. The bottom nickel layers are clearly seen and large uniform nickel 3D structure is achieved.

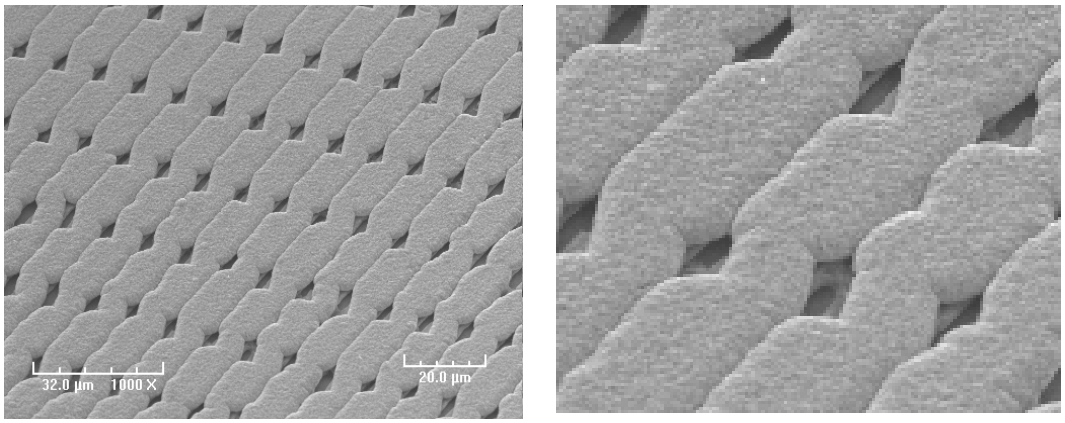

Figure 32 Electroplated nickel 3D structure using template of PMMA 3D structure.

3.4 Summary

In summary, we have developed a novel scheme that allows us to remove the residual layer in thermal nanoimprint without using RIE. In both techniques, the polymer residual layer is first transferred to the surfactant-coated mold surface.

Solvent developing and dewetting are then employed to remove the exposed residual layer on mold protrusions. Both techniques are demonstrated to be successful in removing residual layers in thermal nanoimprint. The elimination of the RIE step in thermal nanoimprint for residual layer removal has significant implications. Firstly, it allows polymer patterning by nanoimprint to be done without the slow and expansive RIE step, which usually limits the overall throughput of and adds extra cost to the nanoimprint process. This enables future up-scaling of nanoimprint technique for continuous production of micro- and nanostructures on polymer films with roller nanoimprint. Secondly, both solvent developing and dewetting are benign to functional polymers. The techniques allow nanoimprint to nondestructively patterning isolated functional polymers. This offers the possibility to use a huge variety of functional polymers, including conducting and semiconducting, piezoelectric, nonlinear optical, magnetic and biodegradable polymers, for miniaturized device and system applications that are currently dominated by inorganic materials. Thirdly, the electroplated nickel 3D structure was demonstrated for using 3D thermoplastic polymer as template to create 3D inorganic structure. It solves great limitation of creating 3D inorganic structure and allows huge opportunity to fabricate further advanced applications. For example, the metallic 3D structures can be used for microfluidic chips for DNA array, medical microsurgical tools and drug delivery. Future extension of the results obtained here to sub-100 nm scale may find important applications in fundamental study of polymer crystallization at a length scale that is comparable to polymer chain length. Finally, advanced 3D scaffolds based on

thermoplastic polymers can be built for advanced applications in bio-MEMS, photonics, electronics and sensor applications.

CHAPTER IV

MULTILAYER PARTICLE SEPARATION SYSTEM

4.1 Introduction

As we have already pointed out in previous chapters, three-dimensional (3D) multilayer polymer microstructures have many applications in electronics, photonics and bioengineering. They are particularly attractive for building multilevel microfluidic channels, which allows for three-dimensional integration of microfluidic components in a lab-on-a-chip system to increase its functionality for biomedical applications. The multilayer microfluidic channels can be easily fabricated by reversal nanoimprint and transfer-bonding under optimized conditions. In this work, we present a lateral flow particle filtration and separation device based on multilayer microfluidic channels with polydimethylsiloxane (PDMS). PDMS has a lot of attractive properties such as low cost, optical transparency, biocompatibility and good permeability to some gases. Such properties enable us to use it for a large variety of microfluidic systems. Recently, researchers presented double-sided molding process to overcome some fabrication problems such as non-uniform surface topography. In this work, we optimize the double sided patterning and transfer-bonding processes to develop a new approach of 3D nano- and micro-PDMS structures. In this device, each layer contains microchannels of different sizes and the channels are stacked on top of each other. When a solution with particles of various sizes flows along the channels in each layer, larger particles will be retained in the top channels, while smaller particles

can migrate into bottom channels shown in Figure 33. Unlike vertical membrane filtration and separation, lateral flow prevents pore clogging and the device can operate continuously for large volume processing. Particles of different sizes can be extracted in each layer. Another significant advantage is that such device allows particles to be separated into multiple size ranges in one run according to the number of the layers and the width of the channels in each layer in the device.

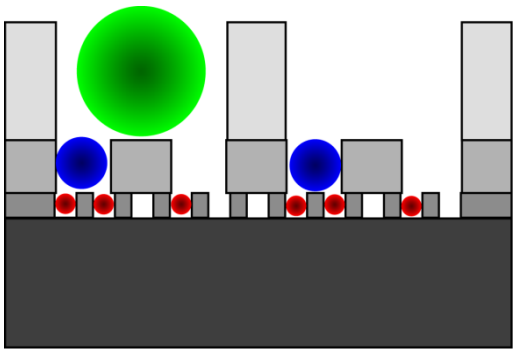

Figure 33. A schematic of the cross-sectional view of the lateral flow particle filtration and separation device based on multilayer microfluidic channels. Colored circles represent particles of different sizes.

4.2 Fabrication of multilayer particle separation system

The multilayer particle filtration and separation device is fabricated by double-side nanoimprint with two different molds [72] and transfer-bonding. The molds for nanoimprint were fabricated from thermally grown silicon oxide wafer by electron-beam lithography or photolithography and RIE. To achieve different size structure at each layer, three different kinds of molds were used for this work: 700 nm pitch and

350nm depth mold, 5 μm pitch and 1μm depth mold, and 10 μm pitch and 1μm depth mold. These molds were coated with FDTS to reduce surface energy for easy mold-releasing and anti-sticking. A PDMS precursor film was coated on Si wafer and then imprinted with mold as shown in Figure 34(a). The imprint temperature was 180^{o}C and the imprint pressure is 5×10^{6} Pa, and the imprinting time was 10 minutes. This patterned PDMS layer will serve as the bottom microchannels of the final device. Instead of directly stacking other layers of PDMS on bottom layer, the second and third layers were fabricated by a double-side imprint process. In double-side nanoimprint, one mold was coated with FDTS and another mold was coated with OTS. The purpose of this is to utilize the difference of adhesion between mold and PDMS layer. Figure 34(b) shows the double-side imprint process at 60^{o}C and 5×10^{6} Pa. for 30 minutes. In this process, the temperature was reduced and the total imprinting time was increased, compared to the previous step, to ensure that there is no residual layer between protrusion areas of both molds. The PDMS layer could stay on the bottom mold after nanoimprint because the surface adhesion between OTS-coated bottom mold and PDMS is much higher than the surface adhesion between FDTS-coated top mold and PDMS. The double-side imprinted PDMS layer on the OTS-coated mold was then transfer-bonded with the first layer as shown in Figure 34(c). To ensure an excellent bonding between two PDMS layers, a brief oxygen plasma treatment was performed on both layers. For this transfer bonding process, only a low pressure of 2×10^{6} Pawas applied at room temperature. In this case, the bonding yield is extremely high. Since PDMS is flexible material, the particles or defects do not affect the yield

significantly and the adhesion between PDMS layers after oxygen plasma treatment is very strong due to covalent bonding. More layers can be added by repeating those steps to construct multilayer PDMS structures. The excellent bonding between the PDMS layers ensures that there is no limitation on how many layers can be added into the device.

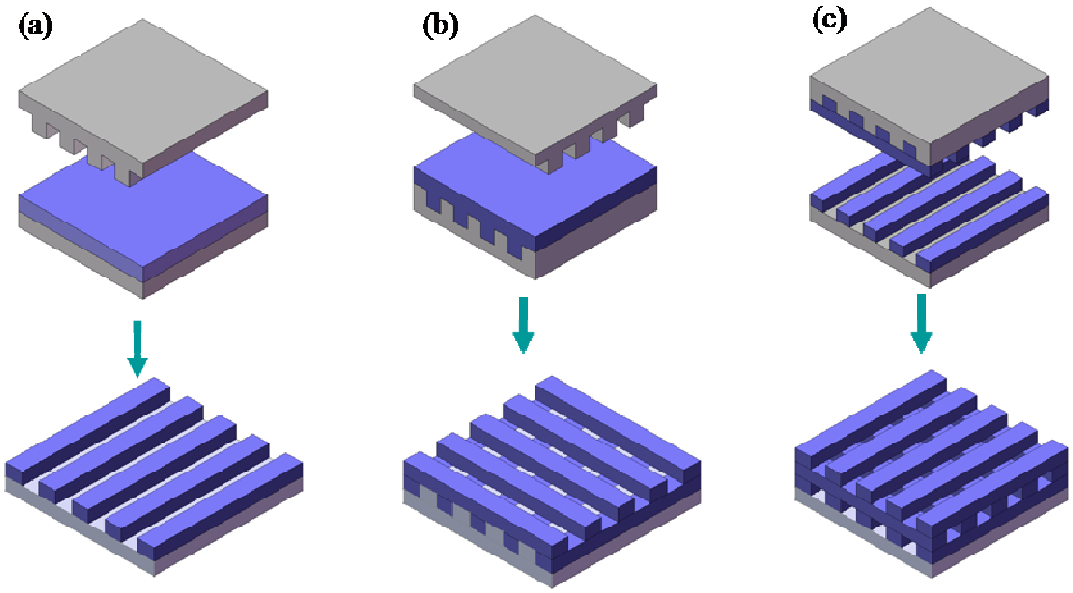

Figure 34. Schematics of the fabrication process for the multilayer PDMS microchannels. (a) Nanoimprint to create the bottom PDMS layer; (b) Double-side imprint with two different molds for middle and top PDMS layers; (c) Transfer-bonding to complete the multilayer device.

Figure 35 shows the multilayer PDMS microfluidic structures obtained by this technique. As shown in Figure 35, there is no residual layer between 10 μm grating

layer and 5 μm grating layer. The PDMS precursor is flowing between two molds during double-side imprinting process. Initially, the PDMS fills out all trench area of both molds and eventually the surplus of PDMS is squeezed out of the molds. As pressure was increased between two molds, the surplus PDMS between protrusion areas of both molds is removed and eventually there is nothing left between protrusion areas. We found that, by controlling pressure and temperature for double-side imprinting process, the thickness of the residual layer can be controlled for other applications. PDMS is a thermoset material so it is very difficult to remove it once it is cured. The permanent PDMS structures can be very useful for filtration and separation applications with stringent particle sorting requirements.

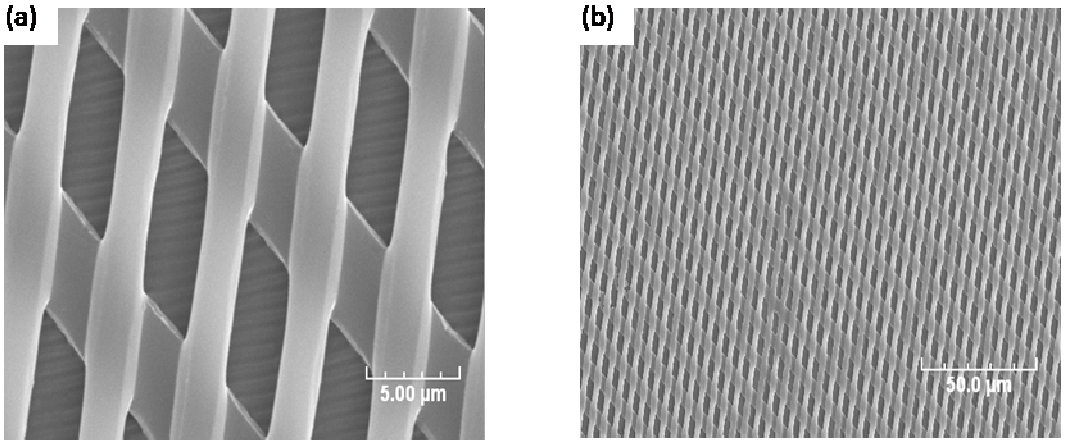

Figure 35. SEM micrographs of multilayer PDMS microfluidic channels. (a) Three-layered PDMS channels. The channel widths in the multilayer structure are 0.35 μm, 5 μm and 10 μm, scale bar 5 μm; (b) A zoom-out view showing the high yield of the fabrication process, scale bar 50 μm.

4.3 Summary

In this work, we developed new method which enables us to build 3D structure with unlimited number of PDMS layers. With this method, structures of different depths and sizes can be combined into one multilayer device. The optimized double-side imprinting process promise controllable residual layer thickness and good patterned structure. Unlike the thermoplastic polymer, the thermoset polymer is extremely difficult to remove the residual layer after curing process. But, we successfully developed the optimized method to remove any residues at contact areas of two molds during curing process. It gives us a lot of opportunity to use thermoset polymers for advanced 3D microfluidic applications. Fully understanding of surfactant coating allows us to control the adhesion of PDMS structure. Such simple process will enable us to open a new approach for time and cost effective application of 3D nano- and micro-fluidic PDMS structure including electronics and bioengineering.

CHAPTER V

POLYMER NANOWIRE FABRICATION BY NANOIMPRINT LITHOGRAPHY

5.1 Introduction

Nanostructure is not only attractive because of its size. Once the size becomes a few nanometers (<100nm), the structure shows special properties which are not observed in bulk sizes. Nanostructure shows unique properties because of its larger surface-to-volume ratio. As its size decreases, the ratio increases. For example, carbon nanotube has 100% ratio of surface area to volume. This means the energy per atom or molecule is higher in nanostructure than in bigger structure since the energy of atoms at surface is higher than that in bulk. This effect can change materials' melting point or increasing catalytic activity [73, 74]. Another interesting effect is quantum size effect [75]. Nano structure is not the bulk, which is composed of thousand of atoms, as well as not a single atom. Since nanostructure exists between single atom, which has discrete energy levels, and the bulk, which has continues energy bands, the optical and electrical properties are different from both single atom and bulk material.

Conventionally, nanostructures can be easily achieved in inorganic materials, such as metals (Au, Ag, etc.) and semiconductors (Si, SiC, InP, etc.), to benefit from their unique properties. Recently, organic nanowires have also gained a lot interests for potentially novel properties. However, the difficulty in achieving polymer

nanowires is limiting their characterizations and applications since none of conventional microelectronic fabrication techniques allows for nondestructive fabrication of polymer nanowires. New fabrication method is greatly desired. Once we can fabricate nanoscale functional polymer wires as shown in Figure 36, we can study their electrical and optical properties.

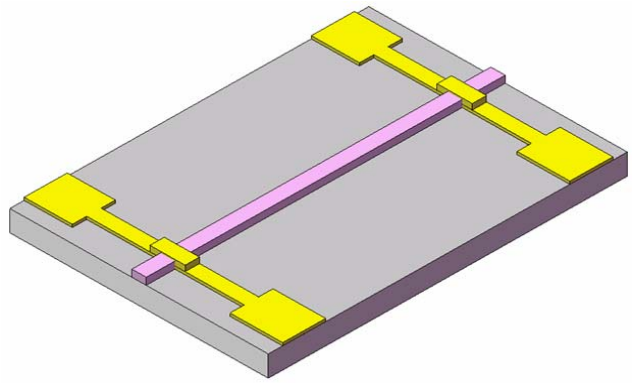

Figure 36. A schematic of isolated nanoscale functional polymer device.

5.2 A novel approach to fabricate nanowire structure by nanoimprint

The residual layer removal technique developed in this dissertation can be used for nondestructive fabrication of polymer nanowires. As shown in Figure 22, after residual layer removal, polymers are embedded in mold trench areas. If the mold structure has a nanoscale dimension, the polymer wires are also in nanoscale. Individual nanowires can be achieved once those polymer wires are detached from mold surface.

The molds for fabricating nanowires were patterned by electron beam lithography on thermal dioxide silicon wafer and followed by RIE. The patterned mold is a 700nm period grating with 350nm depth. In this work, two steps are used to achieve nanowire fabrication. The first step is a combination of solvent developing technique and reversal nanoimprint. According to previous work, the exposed residual layer on the protrusion areas of the mold can be easily removed by solvent developing. And then, the 350nm polymer wires are transferred to a polymer thin film on a substrate by transfer bonding method. The second step is lift-off in a solvent to release individual polymer nanowires. Functional polymers are usually not soluble in acetone unlike PMMA, so functional polymer nanowires can be transferred onto PMMA surface and lift-off in acetone will yield individual nanowires.

5.2.1 Solvent developing and reversal nanoimprint for PMMA nanowire

PMMA with molecular weight of 75000 (T_g = 105˚C) was used as an exemplar polymer in this experiment. The substrate was coated by OTS, which makes the surface of the substrate less hydrophilic for easy releasing. To minimize the residual layer thickness, the starting film thickness was carefully controlled in spin-coating process. By calculating the total volume of trench areas on the mold, the thickness of polymer film can be decided for minimal residual layers after nanoimprint. Because the mold is 1:1 gratings and has a depth of 350nm, the optimal polymer film thickness is 175nm to fill up all trench areas on mold. The mold was coated by FDTS for anti-adhesion layer and easy mold releasing [38]. Only PMMA is used for this work, but

other thermoplastic polymers are also suitable for the techniques developed here. The overall fabrication step is a combination of reversal nanoimprint and solvent developing. First, spin-coated PMMA layer is imprinted with mold by reversal nanoimprint lithography as shown in Figure 15(a). The imprint temperature is 175^{o}C and the imprint pressure is 5×10^{6} Pa. The imprint time is 5 minutes. The detailed reversal nanoimprint and twist-demolding process were fully explained in Chapter II.

Once polymer is transferred onto the mold, the next step is solvent developing to remove residual layer on top of the protrusion areas of mold. This residual removing technique was explained in Chapter III. After removing residual layer, the polymer wires were transferred to another substrate. In this work, the randomly distributed PMMA nanwires was demonstrated as shown in Figure 37.

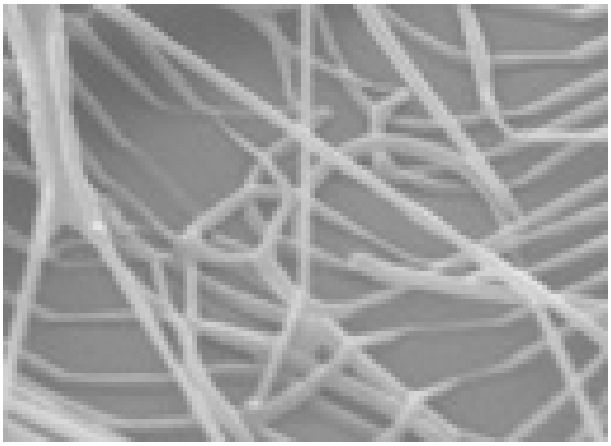

Figure 37 PMMA 350 nm wires on a substrate.

5.2.2 Lift-off for functional polymer nanowire

For functional polymers, we can use lift-off process to strip polymer nanowires from a substrate. First, PMMA was spin-coated on a substrate. P3HT, a conjugated polymer widely used in organic thin-film transistors, sensors and solar cell devices, is spin-coated on the mold directly and then the residual layer at the protrusion area was etched by solvent developing techniques as explained in Chapter III. The P3HT grating structures were transferred onto the PMMA layer at normal imprinting condition, 175^{o}C and 5×10^{6} Pa. The adhesion between PMMA and P3HT is much higher than the adhesion between P3HT and mold so that each P3HT grating is easily transferred onto the PMMA layer. Successfully transferred P3HT layer on top of PMMA, 350nm gratings at left and 5 μm gratings at right, are shown in Figure 38.

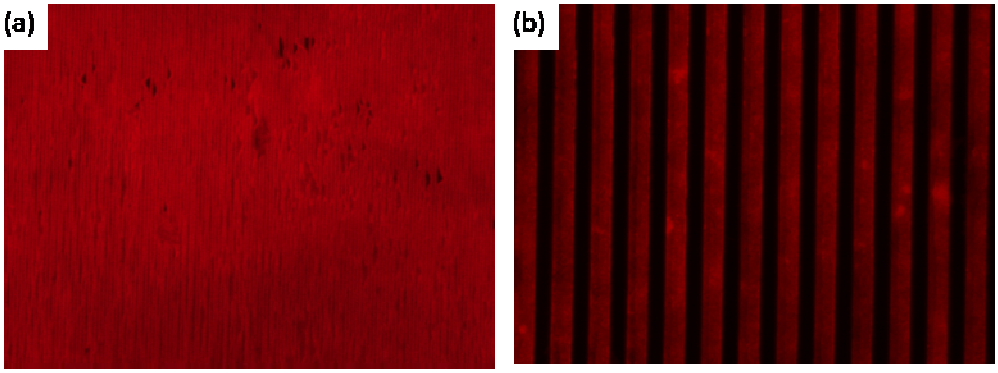

Figure 38 Fluorescent microscope images of P3HT patterns on top of PMMA layer without residual layer. (a) 350 nm gratings and (b) 10 μm gratings.

The next step is to strip P3HT wires from PMMA surface utilizing the solubility difference of the two polymers in acetone. P3HT is not soluble in acetone but PMMA is. The substrate was immersed into acetone for 10 minutes with gentle agitation. All PMMA was dissolved in acetone and P3HT gratings are detached from PMMA film to become individual nanowires. Figure 39 shows fluorescent image of P3HT nanowires after dry the solution.

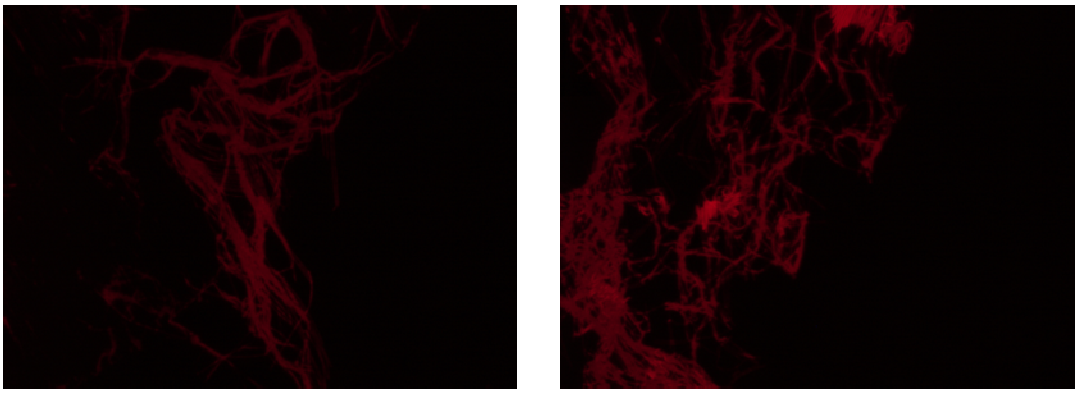

Figure 39. Fluorescent images of P3HT nanowires.

Figure 40 shows the SEM images of the P3HT nanowires. As images shown, the P3HT nanowires clearly detached from PMMA film and individual P3HT nanowires are achieved. This will pave the way for future study of nanowire properties and development of novel application in organic electronics.

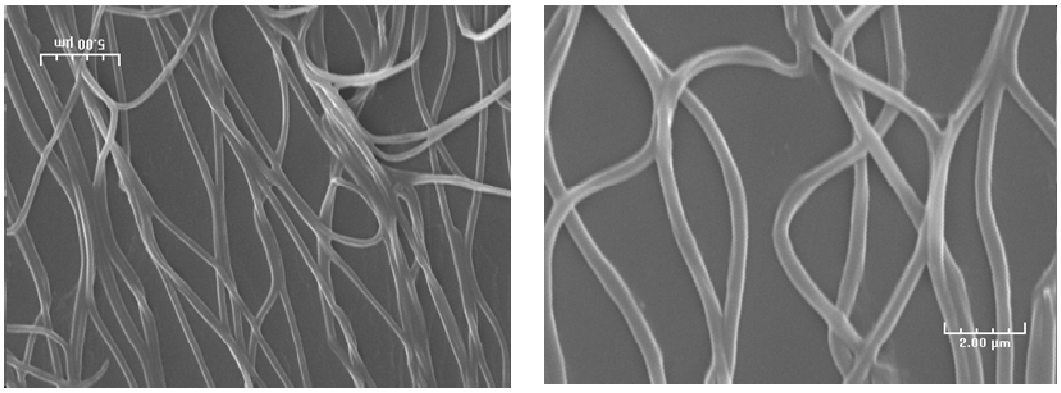

Figure 40. SEM images of P3HT nanowires.

5.3 Summary

In this work, we have developed novel methods which allow us to fabricate polymer nanowire structures. In both methods, solvent developing technique is main reason that this method works. Optimized solvent developing technique can precisely remove the residual layer and left polymers at trench areas only. As mentioned earlier, one of the advantages of thermal nanoimprint lithography is that it can pattern functional polymers without incurring any degradation or damage in those materials. This advantage can be utilized to nondestructively fabricate functional polymer nanowires. Although we only experimented with PMMA and P3HT, this technique is compatible with all polymer materials. Also in this work, we demonstrate only 350nm size nanowires, which is limited by the available molds we have. However, this technique is not limited to this size. Since the polymer nanowire width is determined by the mold structures, sub-100 nm polymer nanowires can be easily achieved if molds with sub-100 nm structures are fabricated. Future work will extend current

results to achieve sub-100 nm polymer nanowires. Since no other fabrication techniques can nondestructively fabricate sub-100nm functional polymer nanostructures, this novel fabrication scheme opens up huge potential of using a variety of functional polymer nanowires in engineering applications. Considering the vast diversity of available functional polymers, such as conducting and semiconducting, piezoelectric, nonlinear optical, magnetic and biodegradable polymers, the fabrication technique develop in this dissertation enable new applications using functional polymer nanowires in variety of areas such as bio-MEMS, photonics, electronics and sensors.

CHAPTER VI

MICROFLUIDIC MDM STRUCTURE AS A TUNABLE OPTICAL FILTER FOR LAB-ON-A-CHIP APPLICATION

6.1 Introduction

Metal-dielectric-metal (MDM) structures can provide resonant enhancement of performance for optoelectronic devices such as light emitting diodes, photodetectors and optical filters [76]. Tunability of the resonant frequency has attracted a lot of research interests due to many important applications such as fluorescence detection of biomaterials. The working principle of MDM structure as an optical filter involves microcavity theory. At the resonance frequency, the electromagnetic field is bounded inside the MDM structure as a standing wave due to the high reflectivity of the metal. The resonance also enhances the coupling of the electromagnetic field on both sides of the filter and results in an enhanced transmission. The resonant frequency is determined by both the thickness and the refractive index of the dielectric layer.

Traditionally, frequency tunability can be realized by changing the dielectric layer thickness using complex micro-electro-mechanical actuators or by applying an electric field to a piezoelectric polymer sandwiched between two metal layers [77]. In this work, we present a novel tuning scheme based on changing the refractive index of the dielectric layer in an MDM structure. The proposed filter device combines a microfluidic channel with an MDM structure (Figure 41). Such configuration allows fluids of different refractive indexes to be transported into and out of the middle

section of the MDM structure through the fluidic channel to achieve frequency tunability. The large index modulation by fluids enables a wide tuning range of resonant frequency.

However, fabricating the MDM structure with microfluidic middle layer is a challenge because the top metal layer cannot be deposited by evaporation. Recently, a fabrication scheme based on nanoimprint and transfer-bonding is developed to create three-dimensional multilayer structures [56]. By using polymer and metal thin films, such method can be adopted to create the desired microfluidic MDM structure.

6.2 Principles of the tunable optical filter

The MDM structure considered here is shown in Figure 41. It consists of two metal layers, which are made of silver due to its high reflectivity and low absorption. A dielectric layer is sandwiched between the metal layers. The dielectric layer thickness is usually around several hundreds of nanometers. It can be either an organic polymer or the air. It can also be a fluid when the microfluidic channel is filled by a liquid.

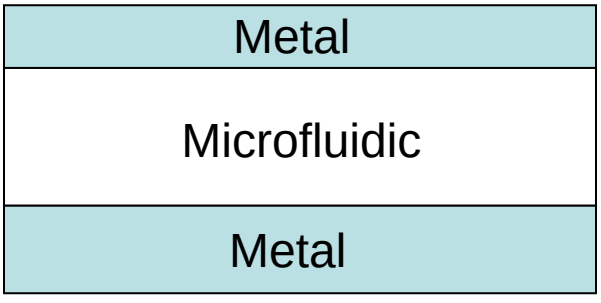

Figure 41. A schematic of the microfluidic MDM structure.

According to the cavity theory [78], the frequencies, at which the resonance and maximum transmission occur, are determined by,

$$\frac{1}{\lambda} = \frac{1}{2nd\cos\theta}\left(m + \frac{\varphi_a + \varphi_b}{2\pi}\right) \qquad m = 0, \pm 1, \pm 2, \ldots$$

where, λ is the optical wavelength in free space, d is the dielectric layer thickness, n is the refractive index, θ is the light incident angle, and φ_a and φ_b are the reflection phase shifts at the metal-dielectric interface.

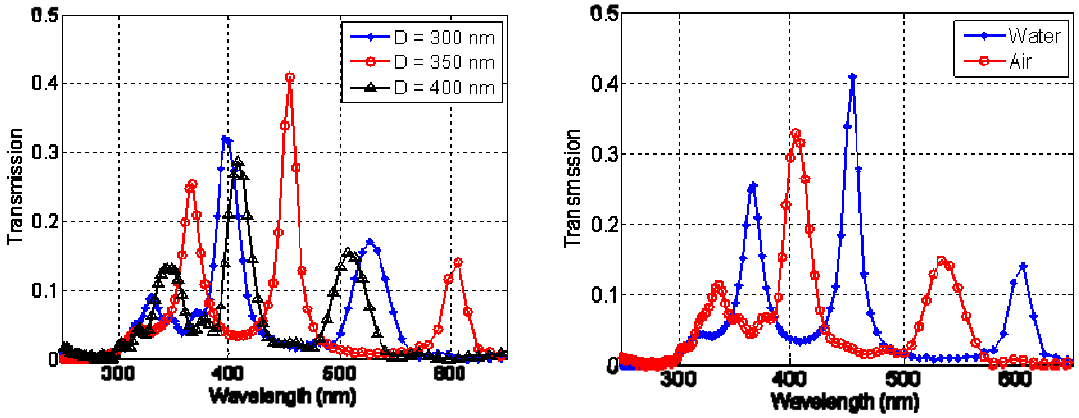

Figure 42. Calculated transmission spectra of MDM structures. (a) transmission spectra for different dielectric layer thickness; (b) transmission spectra of a microfluidic MDM structure with and without water. (Simulated by Huifeng Li)

Figure 42 (a) shows the optical transmission of MDM structures with the dielectric layer thickness (equivalent to the microfluidic channel height) equal to 300 nm, 350 nm, and 400 nm respectively. The resonant frequencies are shifted when the dielectric layer thickness varies. Figure 42 (b) compares the different resonance frequency of the same MDM structure with or without water in the fluidic channels. A

frequency shift occurs when the channels are filled with water, thus achieving tuning capability. Other liquids with different refractive indexes can also be used to add flexibility in resonant frequency tuning.

6.3 Fabrication

Experimentally, we fabricate the microfluidic MDM structure on a glass substrate using nanoimprint lithography and transfer-bonding technique (Figure 43). Chromium (5 nm) and silver (35 nm) are deposited onto the substrate by thermal evaporation, followed by spin-coating a thin layer of PMMA. The thickness of the PMMA layer can be controlled by the spin speed and the concentration of the PMMA solution. Micropattern will be created in the PMMA layer by nanoimprint at 175ºC and at a pressure of 5 MPa (Figure 43(a)). On the other hand, a separate wafer with metal layer to be transfer-bonded is prepared. The wafer is firstly coated with OTS to reduce the polymer-substrate adhesion. Then a thin layer of PMMA is spin-coated on the substrate before evaporation of 5nm nickel and 35nm silver (Figure 43(b)). Due to the reduced adhesion between the PMMA layer and the surfactant coated wafer, the metal layer along with the thin PMMA layer is able to be transferred onto the PMMA patterns on the first substrate by reversal nanoimprint (Figure 43(c)). Removing the OTS coated wafer completes the whole structure. The fabricated microfluidic MDM structure will be characterized with transmission measurements. The tunability of the resonant frequency will be studied by introducing liquids of different refractive indexes into the microfluidic channel.

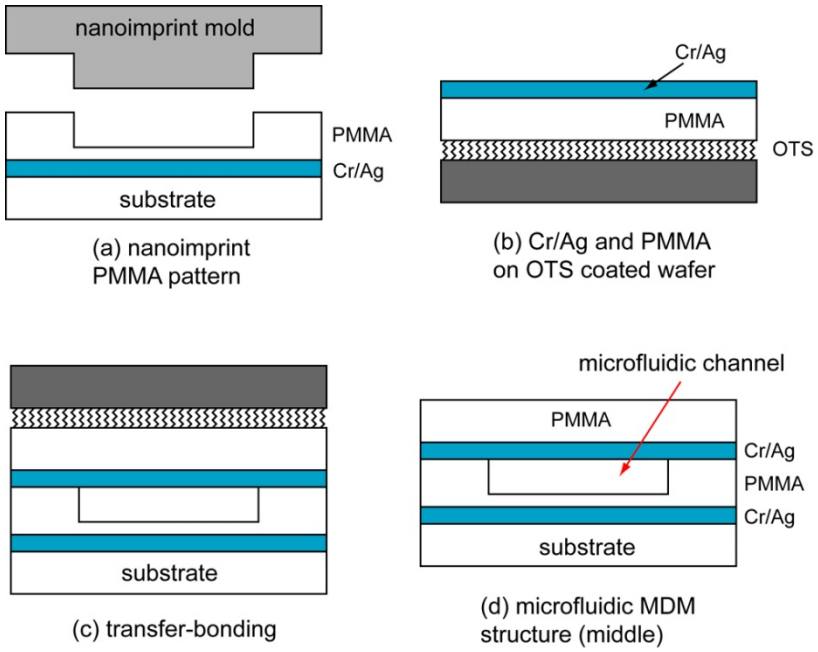

Figure 43. Schematics of the fabrication of the microfluidic MDM structure by nanoimprint and transfer-bonding.

The microfludic MDM structure was successfully fabricated by this method as shown in Figure 44, which are SEM images of the side view (left) and top view (right) of the microfludic MDM structure.

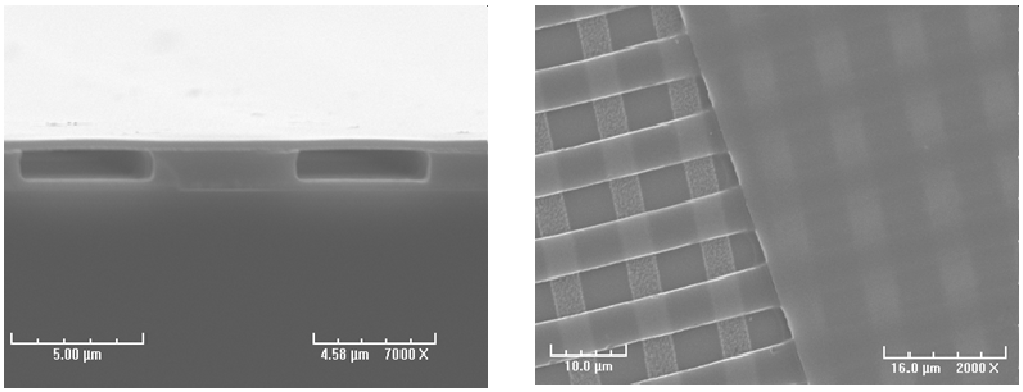

Figure 44. SEM images of the side view (left) and top view (right) of the microfludic MDM structure.

The fabrication scheme we develop here also allows advanced multilayer microfluidic systems to be built. Other components, such as layers containing organic light emitting devices and organic photoconductors can also be integrated into the microfluidic system. The tunable optical filter allows simple tuning of excitation wavelength to selectively excite certain biomolecules tagged with fluorescent dyes, or blocks certain wavelengths from reaching the photodetector when detecting a specific molecule in a mixture. The multilayer integration of light sources, optical filters and optical detectors can yield a portable and ultra-compact lab-on-a-chip system, which is convenient for numerous point-of-care bioanalysis.

6.4 Summary

In conclusion, we proposed here a novel optical filter by introducing microfluidic channels into a conventional MDM structure. The tunable optical filter

can be easily fabricated by nanoimprint and transfer-bonding technique. The performance of the tunable filter is demonstrated by both numerical simulations based on a finite-difference-time-domain algorithm and experimental characterization. Such tunable microfluidic MDM structures can be integrated with organic light emitting devices and organic photoconductors to construct a monolithically integrated fluorescence detection system for lab-on-a-chip applications.

CHAPTER VII

CONCLUSION

As a lithography technique, nanoimprint has gained a huge amount of attention in recent years due to its advantages such as high resolution, high throughput, simplicity and low cost. In principle, nanoimprint is a physical molding or embossing process for patterning soft materials such as polymers. This simple technique has already been demonstrated to have sub-10 nm resolution in both thermal and UV imprint. As a result, nanoimprint is considered as one of the candidates for next generation lithography techniques for future microelectronic fabrication.

3D polymer structures are attractive in many micro- and nanofabricated devices and systems, since the extra structural dimension can provide denser integration and superior performance to accomplish complex tasks. Successful fabrication of three-dimensional multilayer microstructures in thermoplastic polymers using optimized layer-transfer and transfer-bonding techniques are developed. The optimized layer-transfer and transfer-bonding techniques promise high yield, high throughput and good polymer pattern formation. For layer-transfer, twist-demolding ensures good polymer placement on the mold surface for subsequent transfer-bonding. Bonding with a thin adhesive layer and direct thermal bonding near T_g were experimented for polymer transfer-bonding with high yield. Aside from achieving near 100% yield, the thin adhesive layer can also be used to bond heterogeneous materials, such as two different polymers or polymer and inorganic materials, thus making it an

ideal method for creating 3D structures based on polymer-inorganic composite materials. The thickness of the adhesion layer needs to be precisely controlled to avoid filling of the bottom layer patterns. The direct thermal bonding near T_g is a generic method that is suitable for all thermoplastic materials, making it extremely versatile in combining different polymer materials for novel applications. By using a different material or a different pattern in each layer, the multilayer fabrication methods developed in this work allow almost unlimited combination of scenarios, thus provide great flexibility in designing and fabricating 3D multilayer structures with unlimited layers for a broad range of applications. The process yield of multilayer structure fabrication is affected by the existence of particles and the density and sizes of the mold patterns. Upon further improvement of process yield, it is believed that the optimized fabrication methods will spur the application of multilayer structures in electronics, photonics and bioengineering. This approach opens up the possibilities of creating 3D multilayer structures in functional polymers for advanced applications. The capability and flexibility of the techniques developed here are expected to have deep impact on the applications of soft materials such as polymers in micro- and nanofabricated devices and systems.

Although NIL technique is developing rapidly in recent years, there are still issues that need to be addressed for broader adoption of the nanoimprint technique. One of the problems is the residual layer that remains in the polymer pattern after nanoimprint. Conventional approach, oxygen RIE process, to remove the residual layer increases the cost and lowers the overall throughput of the nanoimprint process.

More severely, oxygen RIE can degrade or even damage the functional polymers by breaking the polymer chains with highly energetic oxygen ions. A novel scheme is developed here to remove the residual layer in thermal nanoimprint without using RIE. In both techniques, the polymer residual layer is first transferred to the surfactant-coated mold surface. Solvent developing and dewetting are then employed to remove the exposed residual layer on mold protrusions. Both techniques are demonstrated to be successful in removing residual layers in thermal nanoimprint. The elimination of the RIE step in thermal nanoimprint for residual layer removal has significant implications. Firstly, it allows polymer patterning by nanoimprint to be done without the slow and expansive RIE step, which usually limits the overall throughput of and adds extra cost to the nanoimprint process. This enables future up-scaling of nanoimprint technique for continuous production of micro- and nanostructures on polymer films with roller nanoimprint. Secondly, both solvent developing and dewetting are benign to functional polymers. The techniques allow nanoimprint to nondestructively patterning isolated functional polymers. This offers the possibility to use a huge variety of functional polymers, including conducting and semiconducting, piezoelectric, nonlinear optical, magnetic and biodegradable polymers, for miniaturized device and system applications that are currently dominated by inorganic materials. Thirdly, the electroplated nickel 3D structure was demonstrated for using 3D thermoplastic polymer as template to create 3D inorganic structure. It solves great limitation of creating 3D inorganic structure and allows huge opportunity to fabricate further advanced applications. For example, the metallic 3D structures can be used for

microfluidic chips for DNA array, medical microsurgical tools and drug delivery. Future extension of the results obtained here to sub-100 nm scale may find important applications in fundamental study of polymer crystallization at a length scale that is comparable to polymer chain length. Finally, advanced 3D scaffolds based on thermoplastic polymers can be built for advanced applications in bio-MEMS, photonics, electronics and sensor applications.

Another advantage of nanoimprint is its ability to directly create micro- and nanostructures in functional polymers such as semiconducting and piezoelectric polymers. This is because thermal nanoimprint only needs temperature and pressure for pattern replication, which both are benign to functional polymers. This feature combined with newly developed techniques such as transfer-bonding and residue removal techniques opens up the possibilities in nondestructive patterning of functional polymers at the micro- and nanoscale for novel applications in electronics, optoelectronics, photonics, sensors and bioengineering. The combination of proposed techniques of layer-transfer, transfer bonding and solvent developing to remove residual layers allows novel fabrication of thermoplastic polymer nanowire structures. In this work, we have developed two methods which allow us to fabricate polymer nanowire structures. In both methods, solvent developing technique is main reason that this method works. Optimized solvent developing technique can precisely remove the residual layer and left polymers at trench areas only. Although we only experimented with PMMA and P3HT, this technique is compatible with all polymer materials. Also in this work, we demonstrate only 350nm size nanowires, which is

limited by the available molds we have. However, this technique is not limited to this size. Since the polymer nanowire width is determined by the mold structures, sub-100 nm polymer nanowires can be easily achieved if molds with sub-100 nm structures are fabricated. Future work will extend current results to achieve sub-100 nm polymer nanowires. Since no other fabrication techniques can nondestructively fabricate sub-100nm functional polymer nanostructures, this novel fabrication scheme opens up huge potential of using a variety of functional polymer nanowires in engineering applications. Considering the vast diversity of available functional polymers, such as conducting and semiconducting, piezoelectric, nonlinear optical, magnetic and biodegradable polymers, the fabrication technique develop in this dissertation enable new applications using functional polymer nanowires in variety of areas such as bio-MEMS, photonics, electronics and sensors.

Finally, several applications of three-dimensional multilayer structures fabricated by the techniques developed in this dissertation are demonstrated. The first application is a novel optical filter by introducing microfluidic channels into a conventional MDM structure. The tunable optical filter can be easily fabricated by nanoimprint and transfer-bonding technique. The performance of the tunable filter is demonstrated by both numerical simulations based on a finite-difference-time-domain algorithm and experimental characterization. Such tunable microfluidic MDM structures can be integrated with organic light emitting devices and organic photoconductors to construct a monolithically integrated fluorescence detection system for lab-on-a-chip applications. The second application is a multilayer

microfluidic channels in which each layer has a different channel size. This device can be used for particle separation and filtration based on lateral fluid flow. In this work, we developed new method which enables us to build 3D structure with unlimited number of PDMS layers. With this method, structures of different depths and sizes can be combined into one multilayer device. The optimized double-side imprinting process promise controllable residual layer thickness and good patterned structure. Unlike the thermoplastic polymer, the thermoset polymer is extremely difficult to remove the residual layer after curing process. But, we successfully developed the optimized method to remove any residues at contact areas of two molds during curing process. It gives us a lot of opportunity to use thermoset polymers for advanced 3D microfluidic applications. Fully understanding of surfactant coating allows us to control the adhesion of PDMS structure. Such simple process will enable us to open a new approach for time and cost effective application of 3D nano- and micro-fluidic PDMS structure including electronics and bioengineering.

REFERENCES

[1] Office of Basic Energy Sciences, http://www.nano.gov/html/facts/The_scale_of_things.html, **2005**.

[2] G. E. Moore, *Proceedings of the IEEE* **1998**, *86*, 82.

[3] M. A. McCord, M. J. Rooks, *Handbook of Microlithography, Micromachining and Microfabrication*, IET, Bellingham, WA **1997**.

[4] A. Kumar, G. M. Whitesides, *Science* **1994**, *263*, 60.

[5] Y. Xia, G. M. Whitesides, *Annual Review of Materials Science* **1998**, *28*, 153.

[6] A. Kumar, G. M. Whitesides, *Applied Physics Letters* **1993**, *63*, 2002.

[7] A. B. Hans, B. L. Niels, D. Emmanuel, M. Bruno, *IBM Journal of Research and Development* **1997**, *41*, 159.

[8] Y. Xia, E. Kim, X.-M. Zhao, J. A. Rogers, M. Prentiss, G. M. Whitesides, *Science* **1996**, *273*, 347.

[9] X.-M. Zhao, Y. Xia, G. M. Whitesides, *Advanced Materials* **1996**, *8*, 837.

[10] E. Kim, Y. Xia, G. M. Whitesides, *Nature* **1995**, *376*, 581.

[11] E. King, Y. Xia, X.-M. Zhao, G. M. Whitesides, *Advanced Materials* **1997**, *9*, 651.

[12] S. Y. Chou, P. R. Krauss, P. J. Renstrom, *Science* **1996**, *272*, 85.

[13] M. D. Austin, H. Ge, W. Wu, M. Li, Z. Yu, D. Wasserman, S. A. Lyon, S. Y. Chou, *Applied Physics Letters* **2004**, *84*, 5299.

[14] A. Allan, "The international technology roadmap for semiconductors," *ITRS Conference*, San Francisco, CA, **2008**.

[15] T. Bailey, B. J. Choi, M. Colburn, M. Meissl, S. Shaya, J. G. Ekerdt, S. V. Sreenivasan, C. G. Willson, "Step and flash imprint lithography: Template surface treatment and defect analysis," *Papers from the 44th International Conference on Electron, Ion, and Photon Beam Technology and Nanofabrication*, CA, **2000**, 3572.

[16] J. Taniguchi, Y. Tokano, I. Miyamoto, M. Komuro, H. Hiroshima, *Nanotechnology* **2002**, *13*, 592.

[17] S. W. Pang, T. Tamamura, M. Nakao, A. Ozawa, H. Masuda, *Journal of Vacuum Science & Technology B: Microelectronics and Nanometer Structures* **1998**, *16*, 1145.

[18] T. Haatainen, P. v. Majander, T. Riekkinen, J. Ahopelto, *Microelectronic Engineering* **2006**, *83*, 948.

[19] K. Pfeiffer, M. Fink, G. Ahrens, G. Gruetzner, F. Reuther, J. Seekamp, S. Zankovych, C. M. Sotomayor Torres, I. Maximov, M. Beck, M. Graczyk, L. Montelius, H. Schulz, H. C. Scheer, F. Steingrueber, *Microelectronic Engineering* **2002**, *61-62*, 393.

[20] H. Schulz, D. Lyebyedyev, H. C. Scheer, K. Pfeiffer, G. Bleidiessel, G. Grutzner, J. Ahopelto, "Master replication into thermosetting polymers for nanoimprinting," *Papers from the 44th International Conference on Electron, Ion, and Photon Beam Technology and Nanofabrication*, Rancho Mirage, CA, **2000**, 3582.

[21] D. K. Schwartz, *Annual Review of Physical Chemistry* **2001**, *52*, 107.

[22] J. C. Love, L. A. Estroff, J. K. Kriebel, R. G. Nuzzo, G. M. Whitesides, *Chemical Reviews* **2005**, *105*, 1103.

[23] A. Busnaina, *Nanomanufacturing Handbook*, CRC Press, Boca Raton, FL, **2006**.

[24] M. Beck, M. Graczyk, I. Maximov, E. L. Sarwe, T. G. I. Ling, M. Keil, L. Montelius, *Microelectronic Engineering* **2002**, *61-62*, 441.

[25] D. Y. Khang, H. Kang, T. I. Kim, H. H. Lee, *Nano Letters* **2004**, *4*, 633.

[26] D. Y. Khang, H. H. Lee, *Langmuir* **2004**, *20*, 2445.

[27] Hitachi Global Storage Technologies, http://www.hitachigst.com/hdd/research/storage/pm/FabPatterned.html, **2004**.

[28] S.-W. Ahn, K.-D. Lee, J.-S. Kim, S. H. Kim, J.-D. Park, S.-H. Lee, P.-W. Yoon, *Nanotechnology* **2005**, *16*, 1874.

[29] S. H. Ahn, J.-S. Kim, L. J. Guo, "Bilayer metal wire-grid polarizer fabricated by roll-to-roll nanoimprint lithography on flexible plastic substrate," *Papers from the 46th International Conference on Electron, Ion, and Photon Beam Technology and Nanofabrication*, CO, **2007**, 2388.

[30] D. L. White, O. R. Wood Ii, "Novel alignment system for imprint lithography," *Papers from the 44th International Conference on Electron, Ion, and Photon Beam Technology and Nanofabrication*, CA, **2000**, 3552.

[31] I. Divliansky, T. S. Mayer, K. S. Holliday, V. H. Crespi, *Applied Physics Letters* **2003**, *82*, 1667.

[32] Q. Yan, X. S. Zhao, J. H. Teng, S. J. Chua, *Langmuir* **2006**, *22*, 7001.

[33] B. T. Holland, C. F. Blanford, A. Stein, *Science* **1998**, *281*, 538.

[34] L. R. Bao, X. Cheng, X. D. Huang, L. J. Guo, S. W. Pang, A. F. Yee, *J. Vac. Sci. Technol. B* **2002**, *20*, 2881.

[35] W. Hu, B. Yang, C. Peng, S. W. Pang, *Journal of Vacuum Science & Technology B: Microelectronics and Nanometer Structures* **2006**, *24*, 2225.

[36] P. Abgrall, C. Lattes, V. Conedera, X. Dollat, S. Colin, A. M. Gue, *Journal of Micromechanics and Microengineering* **2006**, *16*, 113.

[37] H. Ooe, M. Morimatsu, T. Yoshikawa, H. Kawata, Y. Hirai, *J. Vac. Sci. Technol. B* **2005**, *23*, 375.

[38] T. Nishino, M. Meguro, K. Nakamae, M. Matsushita, Y. Ueda, *Langmuir* **1999**, *15*, 4321.

[39] X. D. Huang, L. R. Bao, X. Cheng, L. J. Guo, S. W. Pang, A. F. Yee, *J. Vac. Sci. Technol. B* **2002**, *20*, 2872.

[40] B. Yang, S. W. Pang, *J. Vac. Sci. Technol. B* **2006**, *24*, 2984.

[41] W. Zhao, H. Y. Low, P. S. Suresh, *Langmuir* **2006**, *22*, 5520.

[42] M. Nakajima, T. Yoshikawa, K. Sogo, Y. Hirai, *Microelectronic Engineering* **2006**, *83*, 876.

[43] K. Pfeiffer, M. Fink, G. Gruetzner, G. Bleidiessel, H. Schulz, H. Scheer, *Microelectron. Eng.* **2001**, *57-58*, 381.

[44] D. L. Y. Yang, Y. Xie, L. J. Lee, D. L. Tomasko,, *Advanced Materials* **2007**, *19*, 251.

[45] J. A. Forrest, K. Dalnoki-Veress, J. R. Stevens, J. R. Dutcher, *Phys. Rev. Lett.* **1996**, *77*, 2002.

[46] V. Kestelman, R. Veselovsky, R. A. Veselovsky, *Adhesion of Polymers*, McGraw-Hill, New York **2002**.

[47] A. V. Pocius, D. A. Dillard, M. K. Chaudhury, *Adhesion Science and Engineering*, Elsevier, Amsterdam **2002**.

[48] C. C. Ceden?o, J. Seekamp, A. P. Kam, T. Hoffmann, S. Zankovych, C. M. S. Torres, C. Menozzi, M. Cavallini, M. Murgia, G. Ruani, F. Biscarini, M. Behl, R. Zentel, J. Ahopelto, *Microelectronic Engineering* **2002**, *61-62*, 25.

[49] Z. Hu, B. Muls, L. Gence, D. A. Serban, J. Hofkens, S. Melinte, B. Nysten, S. Demoustier-Champagne, A. M. Jonas, *Nano Letters* **2007**, *7*, 3639.

[50] E. Mele, F. Di Benedetto, L. Persano, R. Cingolani, D. Pisignano, *Nano Letters* **2005**, *5*, 1915.

[51] E. Menard, M. A. Meitl, Y. Sun, J. U. Park, D. J. L. Shir, Y. S. Nam, S. Jeon, J. A. Rogers, *Chemical Reviews* **2007**, *107*, 1117.

[52] Z. Hu, G. Baralia, V. Bayot, J.-F. Gohy, A. M. Jonas, *Nano Letters* **2005**, *5*, 1738.

[53] S. J. Kang, Y. J. Park, J. Y. Hwang, H. J. Jwong, J. S. Lee, K. J. Kim, H.-C. Kim, J. Huh, C. Park, *Advanced Materials* **2007**, *19*, 581.

[54] X. Cheng, L. Jay Guo, *Microelectron. Eng.* **2004**, *71*, 277.

[55] T. Borzenko, M. Tormen, G. Schmidt, L. W. Molenkamp, H. Janssen, *Applied Physics Letters* **2001**, *79*, 2246.

[56] H. Park, H. Li, X. Cheng, *Papers from the 46th International Conference on Electron, Ion, and Photon Beam Technology and Nanofabrication* **2007**, *25*, 2325.

[57] M. A. Meitl, Z.-T. Zhu, V. Kumar, K. J. Lee, X. Feng, Y. Y. Huang, I. Adesida, R. G. Nuzzo, J. A. Rogers, *Nat Mater* **2006**, *5*, 33.

[58] X. Feng, M. A. Meitl, A. M. Bowen, Y. Huang, R. G. Nuzzo, J. A. Rogers, *Langmuir* **2007**, *23*, 12555.

[59] H. Sirringhaus, T. Kawase, R. H. Friend, T. Shimoda, M. Inbasekaran, W. Wu, E. P. Woo, *Science* **2000**, *290*, 2123.

[60] A. Sharma, G. Reiter, *Journal of Colloid and Interface Science* **1996**, *178*, 383.

[61] M. Geoghegan, G. Krausch, *Progress in Polymer Science* **2003**, *28*, 261.

[62] W. D. Hakins, *The Physical Chemistry of Surface Films* Reinhold, New York **1952**.

[63] G. Reiter, *Physical Review Letters* **1992**, *68*, 75.

[64] A. Faldi, R. J. Composto, K. I. Winey, *Langmuir* **1995**, *11*, 4855.

[65] C. Redon, F. Brochard-Wyart, F. Rondelez, *Physical Review Letters* **1991**, *66*, 715.

[66] R. Seemann, M. Brinkmann, E. J. Kramer, F. F. Lange, R. Lipowsky, *Proceedings of the National Academy of Sciences* **2005**, *102*, 1848.

[67] K. Y. Suh, J. Park, H. H. Lee, *The Journal of Chemical Physics* **2002**, *116*, 7714.

[68] G. Lu, W. Li, J. Yao, G. Zhang, B. Yang, J. Shen, *Adv. Mater.* **2002**, *14*, 1049.

[69] Z. Zhang, Z. Wang, R. Xing, Y. Han, *Surface Science* **2003**, *539*, 129.

[70] H. Gau, S. Herminghaus, P. Lenz, R. Lipowsky, *Science* **1999**, *283*, 46.

[71] H. Park, H. Li, X. Cheng, *J. Vac. Sci. Technol. B* **2007**, *25*, 2325.

[72] N. Lucas, S. Demming, A. Jordan, P. Sichler, S. Buttgenbach, *Journal of Micromechanics and Microengineering* **2008**, *18*, 075037.

[73] A. P. Alivisatos, *Science* **1996**, *271*, 933.

[74] P. L. Gai, R. Roper, M. G. White, *Current Opinion in Solid State and Materials Science* **2002**, *6*, 401.

[75] V. I. Klimov, A. A. Mikhailovsky, S. Xu, A. Malko, J. A. Hollingsworth, C. A. Leatherdale, H. J. Eisler, M. G. Bawendi, *Science* **2000**, *290*, 314.

[76] H. Shin, M. F. Yanik, S. Fan, R. Zia, M. L. Brongersma, *Applied Physics Letters* **2004**, *84*, 4421.

[77] C. Pinheiro, J. G. Rocha, L. M. Goncalves, S. Lanceros-Mendez, G. Minas, "A tunable fabry-perot optical filter for application in biochemical analysis of human's fluids," *in 2006 IEEE International Symposium on Industrial Electronics*, **2006**, 2778.

[78] H. A. Macleod, *Thin-film Optical Filters*, Institute of Physics, London **2001**.

APPENDIX A

Mold surfactant coating using vapor method

1. Dehydrate sample on hot plate at 150 °C for 5 minutes.
2. Dehydrate glass beaker on hot plate at 150°C for 5minutes.
3. Set hot plate temperature at 80°C.
4. Place sample in the beaker.
5. Drop the surfactant 2 or 3 drops inside beaker and cover it.
6. Wait for 10 minutes.
7. Post bake sample on hot plate at 80°C for 2 minutes.
8. Check the hydrophobicity with drops of water.
9. Clean the beaker with cleanroom paper.

APPENDIX B

Mold surfactant coating using solvent method

1. Dehydrate sample on hot plate at 150 °C for 5 minutes.
2. Prepare 2 beaker of Heptane sovent (100ml)
3. Drop 2 or 3 drops in 1st Heptane beaker
4. Mix the surfactant with Heptane
5. Immerse the sample in 1st Heptane
6. Wait for 10 minutes with gentle agitation.
7. Take out the sample and immerse it in 2nd Heptane beaker.
8. Wait for 5 minutes with gentle agitation.
9. Post bake sample on hot plate at 80°C for 2 minutes.
10. Check the hydrophobicity with drops of water.
11. Clean the beaker with cleanroom paper.

VITA

Hyunsoo Park was born in Daegu, South Korea. After completing his B.S. in electrical engineering at Kyungpook National University, South Korea, in 2003, he received his M.S. degree in electrical engineering at University of Florida, Gainesville, in 2005. He entered the doctoral program in electrical engineering at Texas A&M University in August 2005 and received his Ph.D. degree in May 2009. He can be reached at the following address:

Hyunsoo Park

214 Zachry Engineering Center, TAMU 3128, College Station, TX 77843